

A Delineation of Diketopiperazine Self-Assembly Processes: Understanding the Molecular Events Involved in *N*^ε-(Fumaroyl)diketopiperazine of L-Lys (FDKP) Interactions

Navneet Kaur,[†] Bo Zhou,[†] Fred Breitbeil,[†] Katherine Hardy,[†] Kelly S. Kraft,[‡]
Iva Trantcheva,[‡] and Otto Phanstiel IV^{*,†}

MannKind Corporation, 1 Casper Street, Danbury, Connecticut 06810, and Department of Chemistry, P.O. Box 162366, University of Central Florida, Orlando, Florida 32816-2366

Received July 23, 2007; Revised Manuscript Received October 15, 2007; Accepted October 26, 2007

Abstract: The *N*^ε-fumaroylated diketopiperazine of L-Lys (FDKP, **1**) self-assembles into microparticles that can be used for pulmonary drug delivery. When these particles are formulated with insulin, the resultant powder (Technosphere Insulin) provides a novel prandial insulin therapy. To better understand the self-assembly of **1**, a series of model compounds were synthesized that allowed for the determination of the preferred intramolecular hydrogen-bonding pattern of FDKP. Variable-temperature NMR (CDCl₃) and FTIR studies of acyclic diamides (**3–7a**) and diketopiperazine models (**7b–9d**) revealed the preference of a 10-membered hydrogen bond between one of the diketopiperazine's amido NH and the appended fumaramido-carbonyl (assigned as a "type B" H bond). Molecular modeling studies identified a low energy conformer in the architecture of **1**, which contains two *N*^ε-fumaroylated lysine side chains appended to the diketopiperazine core. The lowest energy form involved a "cooperative" hydrogen bond motif which involved only one of the diketopiperazine amides and had one "arm" involved in a type B motif and the other in a "type A" hydrogen bond (i.e., the fumaramidyl NH H-bonding to the diketopiperazine amide carbonyl). This cooperative hydrogen bond scenario orients the appended fumaryl groups into a distinctive 90° arrangement and is likely involved in its self-assembly into microparticles.

Keywords: Diketopiperazine; self-assembly; cooperative hydrogen bonding; lysine

Introduction

According to the American Diabetes Association, approximately 7% of the U.S. population has diabetes. The classic mode of insulin delivery for diabetic patients involves daily injections. Patient compliance with this regimen remains an issue. Oral dosing of insulin is problematic due to digestion of this bioactive protein in the stomach. Pulmonary delivery of insulin via inhalable insulin technolo-

gies provides a viable alternative to diabetic patients faced with the daily protocol of injections.

The discovery of a fumaramide-diketopiperazine (FDKP, **1**, Figure 1) derivative provides the basis for a novel inhaled insulin, Technosphere Insulin, which is a major advance for diabetic patients.¹ The technology is predicated upon the self-assembly properties of diketopiperazines and their molecular recognition both in solution and in the solid state.^{1–5} Understanding the precise intramolecular contacts of **1** and

* To whom correspondence should be addressed. Mailing address: Department of Chemistry, P.O. Box 162366, University of Central Florida, Orlando, FL 32816-2366. Tel: (407) 823-5410. Fax: (407) 823-2252. E-mail: ophansti@mail.ucf.edu.

[†] University of Central Florida.

[‡] MannKind Corporation.

(1) (a) Steiner, S. S.; Rhodes, C. A.; Shen, G.; McCabe, R. T. Method for making self-assembling diketopiperazine drug delivery system. U.S. Patent 5,503,852, April 2, 1996. (b) Steiner, S. S.; Feldstein, R.; Lian, H.; Rhodes, C. A.; Shen, G. S. Microparticles for lung delivery comprising diketopiperazine. U.S. Patent 6,071,497, June 6, 2000. (c) Poole, T.; Steiner, S. S. Inhalation apparatus. U.S. Patent 7,140,365, November 28, 2006.

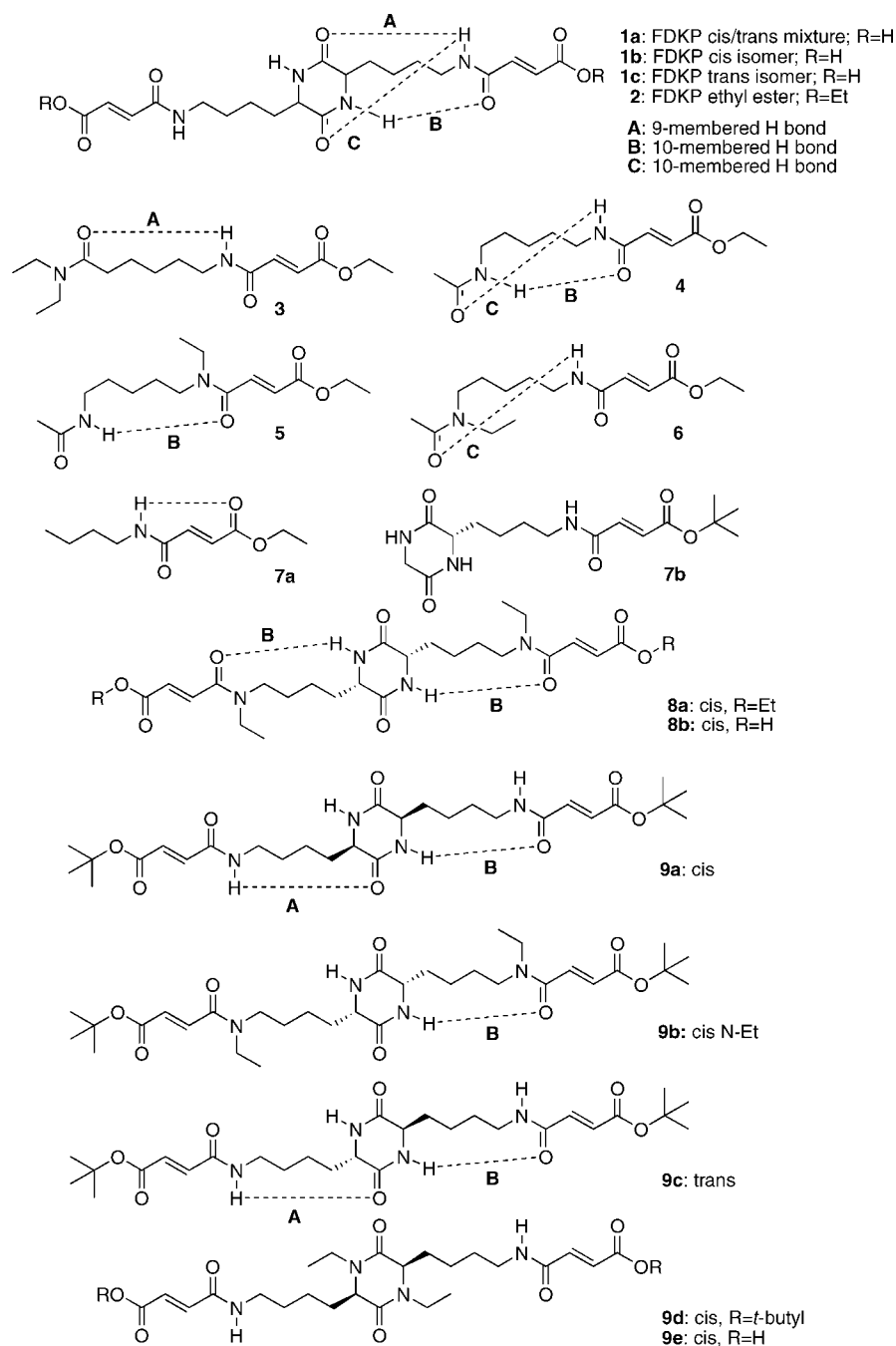


Figure 1. Possible hydrogen-bonding scenarios in FDKP (**1**) and FDKP-OEt (**2**), 9-membered hydrogen bond model **3**, 10-membered hydrogen bond models **4–6**, *N*-butyl fumarate model **7a**, "one-armed" diketopiperazine model **7b**, ethyl ester **8a**, diacid **8b**, *tert*-butyl esters **9a–d**, and diacid **9e**.

identifying the preferred conformation responsible for the self-assembly of **1** into microparticles will assist in the design and development of second-generation inhaled insulin products.^{6–12}

Thus, the relationships between the molecular structure of **1** and the ability of FDKP derivatives to self-associate in the absence of insulin were investigated. This was a reasonable

approach because insulin is adsorbed onto the microparticle as a discreet second step. Unfortunately, the parent tetraamide **1** is extremely insoluble in organic solvents, which makes it a challenging target to study by traditional methods. Even its corresponding diethyl ester **2** (Figure 1) was insoluble in CHCl₃. Therefore, in order to understand the self-assembly behavior of **1**, several models were synthesized which structurally mimic **1** and **2** and yet have better solubility in CDCl₃. Due to their increased solubility, their inter- and intramolecular hydrogen-bonding phenomena were studied via variable-temperature ¹H NMR and FTIR experiments.

(2) Bergeron, R. J.; Phanstiel IV, O.; Yao, G. W.; Milstein, S.; Weimar, W. R. Macromolecular Self-Assembly of Diketopiperazine Tetrapeptides. *J. Am. Chem. Soc.* **1994**, *116*, 8479–8484.

Results and Discussion

Because **1** is known to self-assemble into microspheres,¹ it is likely that the molecule adopts a preferred conformation and then uses intermolecular hydrogen bonds (noncovalent interactions) to establish its self-assembly.¹¹ The hypothesis is that the amide motifs of **1** help generate this special shape and then either through the carboxylic acid groups or the “activated” amide NH the molecule can self-assemble into larger constructs.^{3–5,8,9,11,12}

Within **1**, there are several hydrogen-bonding scenarios which can involve the *N*- ϵ amide group. This group can act as both a hydrogen bond donor via its amide NH group or a hydrogen bond acceptor via its amide carbonyl. Selected conformers of **1**, illustrated in Figure 1, involve a 9-membered ring (**A**) and two 10-membered rings (**B** and **C**), respectively. A series of amido acid derivatives were then designed to identify which of these hydrogen-bonding motifs contribute to the preferred conformation of **1** in hydrophobic environments. Hydrophobic solvents were used in the study because they represent “water-free” environments similar to that experienced by **1** in the pH-driven precipitation step used to create microparticles of **1**. Indeed, when **1** precipitates from solution it undergoes a desolvation step. Therefore, the use of hydrophobic solvents seemed warranted for this type of study, and other authors have utilized these solvents to probe intramolecular contacts within amido acid constructs.¹³

Design. The model compounds were designed to deconvolute the preferred intramolecular hydrogen bond pattern by selectively blocking the other available sites.^{13–16} By studying these materials at low concentration (e.g., 1 mM), intramolecular effects can be observed almost exclusively.¹³ For example, model compound **3**, by design, contains only one hydrogen bond donor (the NH group) and as such has a singular hydrogen bond interaction. An infrared (IR) spectroscopy study conducted at low concentration provided the carbonyl and amide-NH IR frequencies associated with the 9-membered intramolecular hydrogen bond in **3** (**A** in Figure 1).¹³

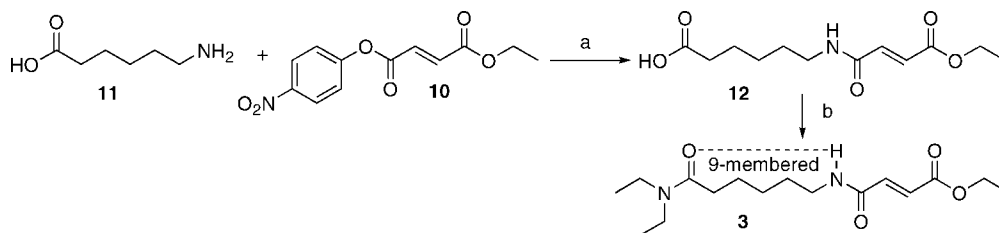
Diamide **4** could adopt either or both of the 10-membered intramolecular hydrogen bonds designated as **B** and **C** in Figure 1. By comparing the IR frequencies observed in **4** with those found with compounds **5** (e.g., model for **B**) and **6** (e.g., model for **C**), the two 10-membered hydrogen-bonding patterns **B** and **C** could be delineated. Compound **7a** was designed to provide information regarding the potential 7-membered hydrogen bond between the fumarate amide NH and ester carbonyl. The other control, “one-armed” **7b**, allowed for an assessment of involvement by the other side chain in **2**.

In diester **8**, the general structure of **2** was maintained, but the 9-membered hydrogen bond (**A**) was blocked by *N*-ethylation of the fumaramide. Because commercial sources of **1** exist as a respective 40:60 mixture of *cis*- and *trans*-diketopiperazine isomers, we synthesized both isomers for independent evaluation. The *cis* isomer was used in **8** and **9**, so as to simplify interpretation of the data. Since **2** was insoluble and therefore was not amenable to our solution studies, we synthesized its related di-*tert*-butyl esters **9a** and **9b**, which had partial solubility in CHCl₃. *Trans* isomer **9c** and the *N*-ethylated diketopiperazine derivatives **9d** and **9e** were synthesized for comparison.

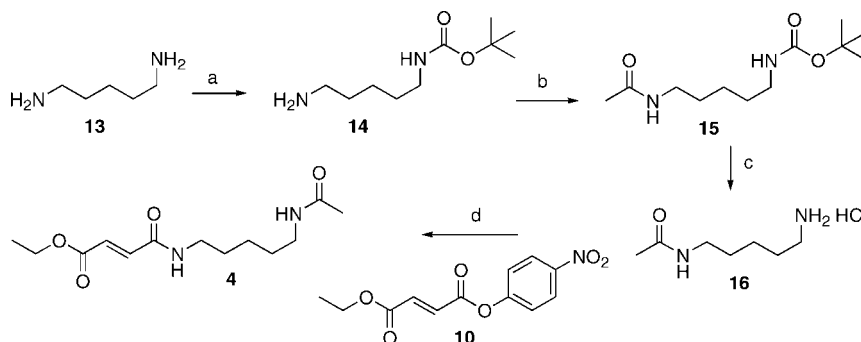
Spectral information from these materials was directly compared to assign the absorbance bands observed in IR

- (3) Luo, T.-J. M.; Palmore, G. T. R. Influence of structure on the kinetics of assembly of cyclic dipeptides into supramolecular tapes. *J. Phys. Org. Chem.* **2000**, *13*, 870–879.
- (4) Palacin, S.; Chin, D. N.; Simanek, E. E.; MacDonald, J. C.; Whitesides, G. M.; McBride, M. T.; Palmore, G. T. R. Hydrogen-Bonded Tapes Based on Symmetrically Substituted Diketopiperazines: A Robust Structural Motif for the Engineering of Molecular Solids. *J. Am. Chem. Soc.* **1997**, *119*, 11807–11816.
- (5) Palmore, G. T. R.; McBride, M. T. Engineering layers in molecular solids with cyclic dipeptide of (S)-aspartic acid. *J. Chem. Soc., Chem. Commun.* **1998**, 145–146.
- (6) Bergeron, R. J.; Yao, G. W.; Erdos, G.; Milstein, S.; Gao, F.; Weimar, W. R.; Phanstiel, O., IV. An Investigation of the Impact of Molecular Geometry upon Microcapsule Self-Assembly. *J. Am. Chem. Soc.* **1995**, *117*, 6658–6665.
- (7) Bergeron, R. J.; Yao, G. W.; Erdos, G. W.; Milstein, S.; Gao, F.; Rocca, J.; Weimar, W. R.; Price, H. L.; Phanstiel, O., IV. The Influence of Molecular Conformation Upon the Self-Assembly of Cyclohexane Diamide Diacids. *Bioorg. Med. Chem.* **1997**, *5* (11), 2049–2061.
- (8) Matsui, H.; Gologan, B.*; Schaffer, H.; Adar, F.; Seconi, D.; Phanstiel, O., IV. Mechanism of Crystalline Dicarboxamide Microsphere Self-Assembly Probed by In Situ Raman Microscopy and Raman Imaging. *Langmuir* **2000**, *16*, 3148–3153.
- (9) Phanstiel, O., IV; Erdos, G. W.; Lachicotte, R. J.; Torres, D.; Richardson, M.; Matsui, H.; Schaffer, H.; Adar, F.; Seconi, D. Nanoconstruction Using Proton-Induced Phase Transitions: Molecular Self-Recognition by Diamide Diacids in Aqueous Environments. *Chem. Mater.* **2001**, *13*, 264–272.
- (10) Breitbeil, F.; Phanstiel, O., IV. Molecular modeling of the 1,1-Cyclopropane and 1,1-Cyclobutane-dicarboxamide Systems: Insights into the Self-Assembly of Diamide Diacids in Water. *Struct. Chem.* **2002**, *13*, 443–453.

- (11) Krische, M. J.; Lehn, J.-M. The Utilization of Persistent H-Bonding Motifs in the self-Assembly of Supramolecular Architectures. *Struct. Bonding (Berlin)* **2000**, *96*, 3–29.
- (12) Burrows, A. D. Crystal Engineering Using Multiple Hydrogen Bonds. *Struct. Bonding (Berlin)* **2004**, *108*, 55–96.
- (13) Gung, B. W.; Zhu, Z.; Zou, D.; Everingham, B.; Oyeamalu, A.; Crist, R. M.; Baudlier, J. Requirement for Hydrogen-Bonding Cooperativity in Small Polyamides: A Combined VT-NMR and VT-IR Investigation. *J. Org. Chem.* **1998**, *63*, 5750–5761.
- (14) Gellman, S. H.; Dado, G. P.; Liang, G.; Adams, B. R. Conformation-directing effects of a single intramolecular amide-amide hydrogen bond: variable-temperature NMR and IR studies on a homologous diamide series. *J. Am. Chem. Soc.* **1991**, *113*, 1164–1173.
- (15) Dado, G. P.; Gellman, S. H. Intramolecular Hydrogen Bonding in Derivatives of beta-Alanine and gamma-Amino Butyric Acid; Model Studies for the Folding of Unnatural Polypeptide Backbones. *J. Am. Chem. Soc.* **1994**, *116*, 1054–1062.
- (16) Stevens, E. S.; Sugarwa, N.; Bonara, G. M.; Toniolo, C. Conformational analysis of linear peptides. 3. Temperature dependence of NH chemical shifts in chloroform. *J. Am. Chem. Soc.* **1980**, *102*, 7048–7050.

Scheme 1^a

^a Reagents: (a) Na₂CO₃/THF; (b) diethylamine/BOP/CH₂Cl₂.

Scheme 2^a

^a Reagents: (a) DTBD/TEA/MeOH; (b) CH₃COCl/TBA-HSO₄/K₂CO₃/CH₂Cl₂; (c) 4 N HCl, 0 °C; (d) TEA/Na₂CO₃/THF, 0 °C.

experiments. In short, by comparing the IR frequencies of the acyclic and diketopiperazine models, the preferred hydrogen-bonding patterns of **1** and **2** were identified. In addition, molecular modeling facilitated the assignment of a cooperative hydrogen bond, wherein both types **A** and **B** were operative within this tetra-amide architecture and required the use of both side-chain “arms” of the diketopiperazine.

In addition, ¹H NMR investigations were performed to observe how the amide NH chemical shift was altered as a function of temperature. Large temperature dependencies indicated that intramolecular hydrogen bonds were indeed in play with many of these motifs. The IR and NMR findings are reported below.

Synthesis. Compounds **3–9** were synthesized as models for FDKP interactions. Scheme 1 shows the synthesis of compound **3**, in which 6-aminohexanoic acid (**11**) was *N*-acylated with ethyl *p*-nitrophenyl fumarate **10** to give compound **12** in 62% yield. Further coupling with diethylamine using the BOP reagent¹⁷ gave compound **3** in 84% yield.

As shown in Scheme 2, 1,5-diaminopentane (**13**) was converted to its *N*¹-Boc derivative **14** by using commercially available di-*tert*-butyl dicarbonate (DTBD), and **14** was then *N*⁵-acylated with acetyl chloride using K₂CO₃/TBA-HSO₄ in CH₂Cl₂ to give compound **15** in 75% yield. Deprotection

of the Boc group by 4 N HCl gave compound **16** as its HCl salt, which was then acylated with ethyl(*p*-nitrophenyl)fumarate **10** to give compound **4** in 56% yield.

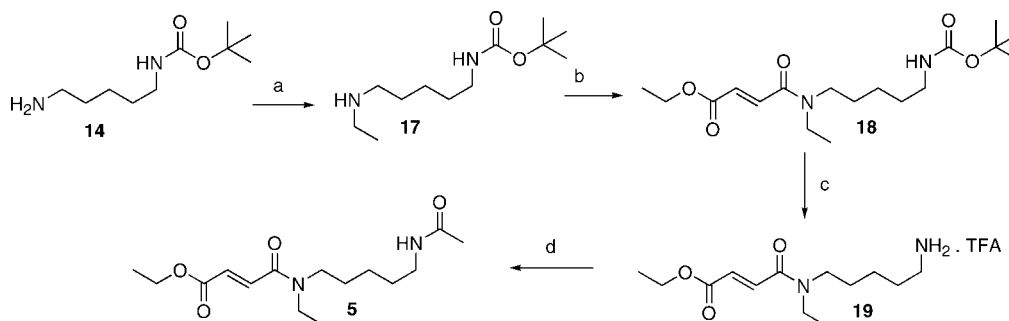
Alternatively, compound **14** was *N*-alkylated with ethyl bromide to give compound **17** (Scheme 3). Compound **17** was acylated with ethyl *p*-nitrophenyl fumarate **10** at –60 °C in the presence of Na₂CO₃ to give amide **18** in 80% yield. Removal of the Boc group with 50% TFA/CH₂Cl₂ and subsequent *N*-acylation with acetyl chloride resulted in the diamide ester **5** in 77% yield.

As shown in Scheme 4, reductive amination of Boc-protected pentylamine (**14**) with benzaldehyde gave the *N*-benzylamine derivative **20** in 68% yield, which was further *N*-alkylated with ethyl bromide to give tertiary amine **21** in 95% yield. Removal of the benzyl group by hydrogenation over 10% Pd–C in ethanol resulted in monoethylated secondary amine **17**, which was acylated with acetyl chloride to give compound **22a** in 65% yield. Deprotection of the Boc group by trifluoroacetic acid provided **22b**, which was further *N*-acylated with **10** to give diamide **6** in 60% yield.

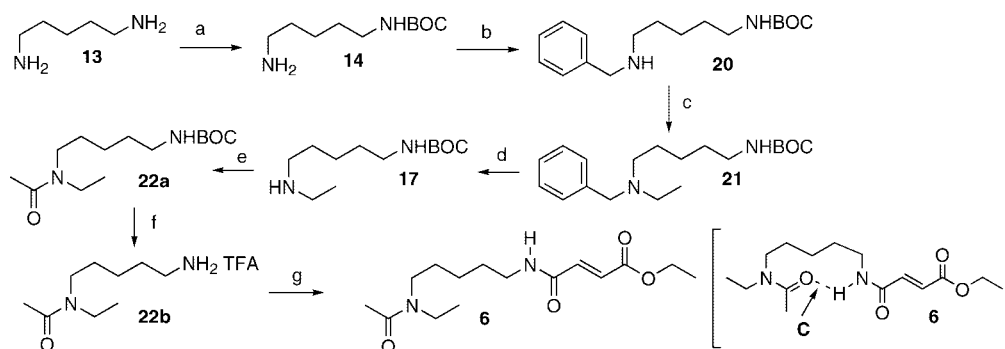
As shown in Scheme 5, control **7a** was synthesized in one step via the *N*-acylation of *n*-butylamine with **10** to give amide **7a** in 70% yield. Control **7b** was synthesized via stepwise construction of Gly-(*N*^ε-Cbz)-L-Lys diketopiperazine **23c**. The amide **23a** was formed by coupling of glycine ethylester with *N*^α-Boc, *N*^ε-Cbz-L-Lys using dicyclohexylcarbodiimide (DCC).¹⁸ Boc-group removal and cyclization of **23a** gave the Cbz-protected diketopiperazine **23b**, which

(17) Castro, B.; Dormoy, J. R.; Evin, G.; Selve, C. Reactifs de couplage peptidique I (1) - l'hexafluorophosphate de benzotriazolyl N-oxytrisdiméthylamino phosphonium (B.O.P.). *Tetrahedron Lett.* **1975**, 1219–1222.

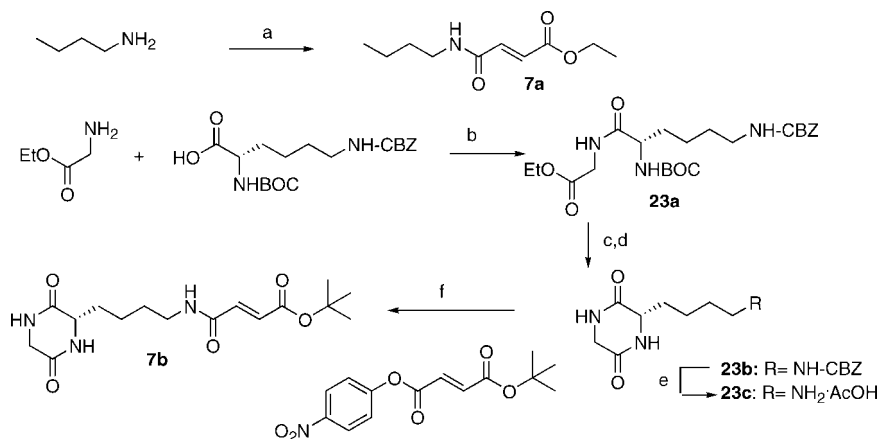
(18) Sheehan, J. C.; Hess, G. P. A New Method of Forming Peptide Bonds. *J. Am. Chem. Soc.* **1955**, 77, 1067–1068.

Scheme 3^a

^a Reagents: (a) ethyl bromide/K₂CO₃/CH₃CN; (b) **10**, Na₂CO₃/THF; (c) 50% TFA/CH₂Cl₂; (d) acetyl chloride, K₂CO₃/TBA-HSO₄/CH₂Cl₂.

Scheme 4^a

^a Reagents: (a) DTBD/TEA/MeOH; (b) benzaldehyde/MeOH/CH₂Cl₂; NaBH₄; (c) EtBr/CH₃CN/K₂CO₃, 60 °C; (d) 20% Pd-C/EtOH; (e) CH₃COCl/K₂CO₃/TBA-HSO₄/CH₂Cl₂; (f) TFA, 0 °C g) **10**, aq Na₂CO₃/CH₂Cl₂.

Scheme 5^a

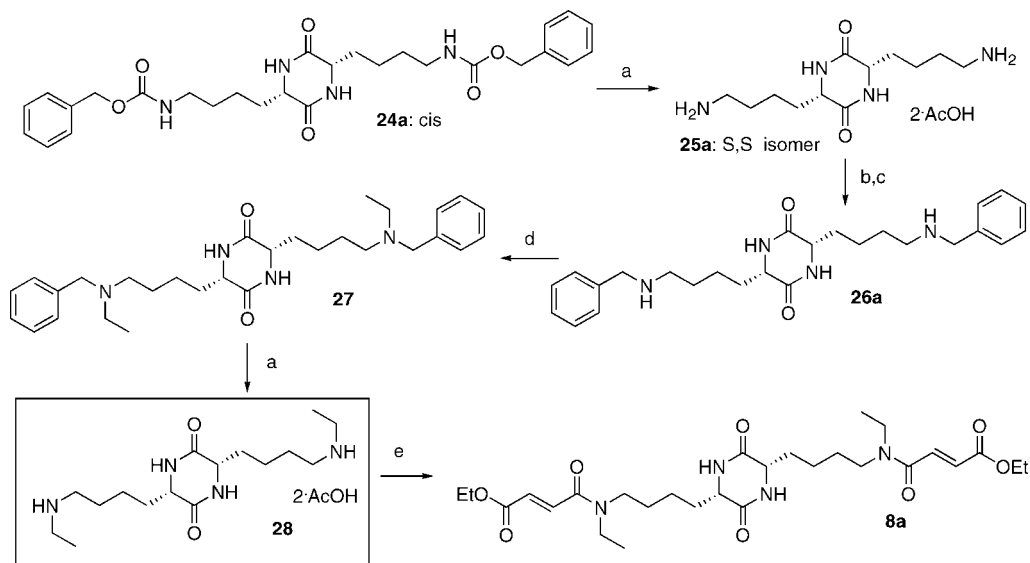
^a Reagents: (a) **10**, aq Na₂CO₃; (b) DCC; (c) 50% TFA/CH₂Cl₂; (d) AcOH, NMM, butanol; (e) H₂ gas, Pd-C, AcOH; (f) aq Na₂CO₃.

was deprotected using H₂ gas and Pd-C to give the amine salt **23c**, which was acylated to give the triamide **7b**.

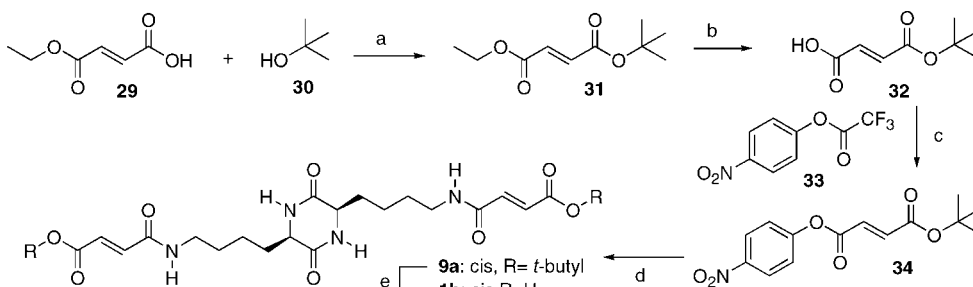
For the synthesis of compound **8**, the *cis*-Cbz-protected diketopiperazine **24a** was used.^{2,16} Deprotection of the (*S,S*)-benzyl carbamate **24a** by H₂ gas and 10% Pd-C in acetic acid/CH₂Cl₂ resulted in the acetic acid salt of the diamine **25a**. As shown in Scheme 6, reductive amination of compound **25a** with benzaldehyde gave the *N*-benzylamine derivative **26a** in 76% yield, which was further *N*-alkylated

with ethyl bromide to give compound **27**. Removal of the *N*-benzyl group by hydrogenation over 10% Pd-C resulted in the secondary amine **28**. Note: the intermediary *N*-benzylation/debenzylation steps facilitated both the yield and isolation of the monoethylated amine targets. In the final step, **28** was *N*-acylated with **10** to give compound **8a** in 54% yield.

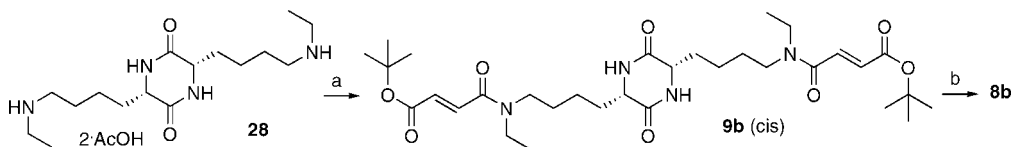
As shown in Scheme 7, monoethyl fumarate **29** was coupled with *tert*-butyl alcohol **30** using DCC to provide

Scheme 6^a

^a Reagents: (a) 10% Pd–C/CH₃COOH/CH₂Cl₂; (b) benzaldehyde/TEA/MeOH/CH₂Cl₂; (c) NaBH₄/MeOH/CH₂Cl₂; (d) EtBr/K₂CO₃/CH₃CN; (e) **10**, Na₂CO₃/THF/TEA.

Scheme 7^a

^a Reagents: (a) DCC/DMAP/CH₂Cl₂; (b) 1 M NaOH/THF; (c) *p*-nitrophenyl trifluoroacetate **33**/TEA; (d) **25b**, TEA/Na₂CO₃/THF; (e) 50% TFA/CH₂Cl₂.

Scheme 8^a

^a Reagents: (a) **34**, aq Na₂CO₃, THF; (b) 50% TFA/CH₂Cl₂.

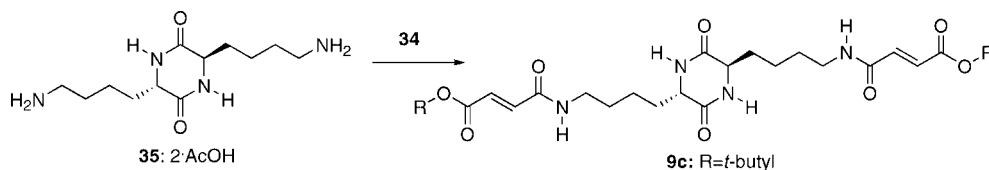
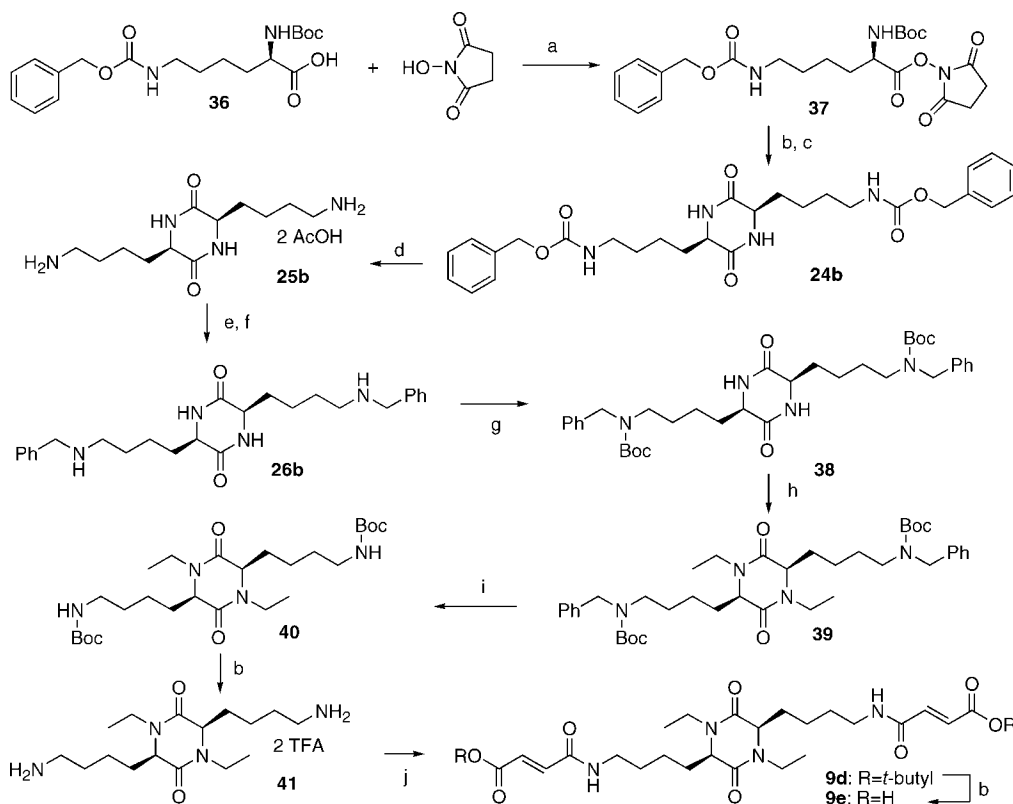
tert-butyl ethyl fumarate **31**. Selective hydrolysis of the ethyl ester using NaOH gave acid **32** (upon workup) in 80% yield, which upon transesterification with **33** provided *p*-nitrophenyl *tert*-butyl fumarate **34** in 89% yield. Compound **25b** (the *R,R* enantiomer of **25a**) was *N*-acylated with **34** to generate *cis* di-*tert*-butyl ester **9a** in 44% yield. Although **9a** was the enantiomer of the *S,S* form, it could be used to provide valuable spectral data for comparisons. Compound **9b** (*S,S* form) was synthesized from the bis secondary amine **28** using the activated fumarate ester **34** in 68% yield (Scheme 8).

Deprotection of the *tert*-butyl esters **9a** and **9b** provided the respective *cis* acids **1b** and **8b** in good yield using

trifluoroacetic acid (TFA) and CH₂Cl₂. The *trans* isomer **9c** was synthesized from the acetic acid salt of *trans*-diketopiperazine of lysine **35** (Scheme 9).

As shown in Scheme 10, the synthesis of compounds **9d** and **9e** began with activated ester **37**, which was synthesized from commercially available Boc-*N*^ε-Z-D-lysine **36** and *N*-hydroxysuccinimide using DCC as the coupling agent. Removal of the Boc group of **37** with TFA and intermolecular cyclization in pyridine provided diketopiperazine **24b** in 69% yield. The Cbz groups were removed by H₂, and reductive amination of amine **25b** with benzaldehyde gave secondary amine **26b**, which was protected using di-*tert*-butyl dicarbonate to obtain compound **38**. *N*-Ethylation of

Scheme 9

Scheme 10^a

^a Reagents: (a) DCC, THF; (b) 50% TFA/CH₂Cl₂; (c) pyridine; (d) 10% Pd–C/H₂/CH₃COOH/CH₂Cl₂; (e) benzaldehyde/TEA/MeOH/CH₂Cl₂; (f) NaBH₄/MeOH/CH₂Cl₂; (g) di-*tert*-butyl dicarbonate/TEA; (h) EtBr/NaH/THF; (i) 10% Pd–C/H₂/EtOH; (j) **34**, aq Na₂CO₃/THF.

38 by NaH and EtBr gave compound **39** in 70% yield. Successive removal of the *N*-benzyl and Boc groups resulted in the primary amine **41** as its TFA salt, which upon acylation with *tert*-butyl *p*-nitrophenyl fumarate **34** gave *tert*-butyl ester **9d** in 87% yield. Removal of the *tert*-butyl ester of **9d** (50% TFA/CH₂Cl₂) gave acid **9e** in 99% yield.

Once synthesized, these model compounds were evaluated by ¹H NMR and IR measurements using the methods of Gung et al.¹³

Variable-Temperature ¹H NMR Studies (VT-NMR). Understanding the effects of solvation by an organic solvent is a key step in understanding the process of the self-assembly of **1**. In terms of solvation effects, an organic solvent like CDCl₃ provides an opportunity to study these systems in an intermediate environment somewhere between the crystalline and dissolved states. Due to the lack of solubility of **1** in CDCl₃, the soluble models (**3–9**, with the exception of **8b**) were used.

Specifically, ¹H NMR studies determined the temperature dependence of the amide NH chemical shift (δ NH) in ppb/K (as measured in CDCl₃) for the model derivatives (Figure 1). Variable-temperature ¹H NMR experiments (VTNMR) provided a plot of NH chemical shift versus temperature (in K); the slope of which is expressed in ppb/K. A large absolute value of the slope (>6 ppb/K) implies that the hydrogen bond is undergoing a change in environment through the temperature range studied, while a small value (1–2 ppb/K) denotes a hydrogen bond which remains bonded or in its unbound state throughout the temperature range.¹³

For example, an intramolecular hydrogen bond may break over the course of the temperature range. This event would significantly alter the chemical shift of the NH signal and give a large negative slope (–6 ppb/K), whose absolute value (6 ppb/K) reflects this dramatic change as a function of temperature. In contrast, the ¹H NMR chemical shift of a solvent-exposed or “free” NH would undergo little change as a function of temperature (because its bonding partner

Table 1. Variable-Temperature ^1H NMR Data for Selected Models

compd	slope (ppb/K) expressed as absolute value
3	7.5
4-1	5.2
4-2	3.8
5-1	5.5
5-2	3.6
6	7.9
7a	2.8
7b-1	8.0
7b-2	4.8
7b-3	4.4
8a-1	9.4
8a-2	9.6
8a-3	9.8
8a-4	8.8
9a-1	10.4
9a-2	10.6
9b-1	10.6
9b-2	6.5
9b-3	5.9
9b-4	4.7
9c-1	6.3
9c-2	4.8
9d	5.4

does not change) and would give a relatively flat slope (-2 ppb/K), whose absolute value (2 ppb/K) would reflect this limited dependency on temperature.^{13–16} The results of the temperature dependence on NH chemical shift of selected models (each at 1 mM in CDCl_3) are listed in Table 1.

Compound **3** having only 9-membered hydrogen bonding between the fumaramide NH and amide carbonyl (designated as **A** in Figure 1) shows a slope with absolute value of 7.5 ppb/K, which is consistent with the intramolecular hydrogen bond **A**. It was assigned as an intramolecular bond due to the dilute concentration (1 mM compound in CDCl_3) used in these measurements.

Two NH populations (Table 1: **4-1** and **4-2**) were observed with the diamide motif **4** and gave absolute values of $\Delta\text{ppb/K}$ of 5.2 and 3.8 ppb/K, respectively. These are intermediary values and suggest at least one intramolecular hydrogen bond may be in play. This may stem from either or both of the two possible 10-membered hydrogen bonds (designated as **B** and **C** in Figure 1). Compound **5** also gave two NH populations (**5-1** and **5-2**) in the ^1H NMR spectrum, respectively. Since **5** only has one NH available for hydrogen bonding, it suggests that this NH exists in part as a solvent-exposed free NH (**5-2**, 3.6 ppb/K) and an intramolecularly bound NH (5.5 ppb/K). Note the similar temperature dependencies as **4**. In contrast, compound **6**, which also has a singular NH, gave one NH population in the ^1H NMR spectrum (7.9 ppb/K). This is consistent with an intramolecular hydrogen bond of type **C** in Figure 1.

When comparing the ppb/K values of compounds **4–6**, compound **6** shows the highest value 7.9 ppb/K and a singular NH population, while both **4** and **5** gave (at least) two NH populations. Moreover, when one looks at **4**, where both the intramolecular **B** and **C** options are available, the magnitude of the value of the hydrogen bond found in **4** (5.2 ppb/K) is more consistent with the $\text{N-H}\cdots\text{O}=\text{C}$ bond observed in **5** (**B**: 5.5 ppb/K). Thus, although both **B** and **C** are viable options for the NH's of compound **4**, the NMR data suggested that **B** is the preferred interaction in **4**. The remaining NH population in **4** (i.e., **4-2**) had a temperature dependence of 3.8 ppb/K and is apparently solvent-exposed.

The low 2.8 ppb/K value observed with the lone NH population of compound **7a** suggests that there is no intramolecular hydrogen bonding between ester carbonyl and amide NH to form a 7-membered ring in compound **7a**.¹³ This seems reasonable because the trans alkene motif of the fumarate group does not facilitate close contact of the amide NH and ester carbonyl groups. In this manner, **7a** was a good model for the behavior of the free fumaramide NH at 1 mM.

Since the acyclic models **3–7a** did not contain the central diketopiperazine ring system, they may not be the ideal models for **1**. However, they did allow for the respective ^1H NMR chemical shifts and IR frequencies to be assigned for particular H-bond interactions and suggested that “type **B**” hydrogen bonding was preferred. In addition, the soluble diketopiperazine models of **2** (**7b**, **8a**, **9a–d**) provided more insight into the unique bonding environment of the parent system.

As shown in Table 1, VT-NMR experiments with the one-armed control **7b** (1 mM in CDCl_3) gave three NH populations with 8.0, 4.8, and 4.4 ppb/K, respectively. Since **7b** has only one side-chain “arm”, the high temperature dependence must be from one of the possible intramolecular bonds (types **A** or **B** or **C**) and the lower dependencies from the free NH. These are clearly not from “interchain interactions” (i.e., chain to chain contacts within the same molecule) due to the “one-armed” structure of **7b**.

In compound **8a**, 9-membered hydrogen bond **A** and 10-membered hydrogen bond **C** are blocked by *N*-ethylation of the fumaramide. This leaves only 10-membered hydrogen bond **B** available. By blocking the **A** and **C** bonding patterns, there was a dramatic change in the solubility of compound **8a**, which is freely soluble in CDCl_3 , whereas **2** is insoluble in CDCl_3 . *This dramatic change in the solubility property by itself suggests that the fumaramide NH is responsible for establishing intermolecular contacts and facilitates self-aggregation.*

Interestingly, compound **8a** in 1 mM solution shows four NH populations. All four populations had high ppb/K values (≥ 8.8 ppb/K at 1 mM) suggesting that they are all involved in intramolecular bonds. Their assignments were confirmed by adding D_2O , which caused the NH signals to disappear in the NMR spectrum. Inspection of the molecule **8a** suggests that type **B** hydrogen bonding should dominate. We speculate that the four NH signals are generated by cis–trans isomerism of the tertiary amide group. Indeed, other *N*-alkylamides

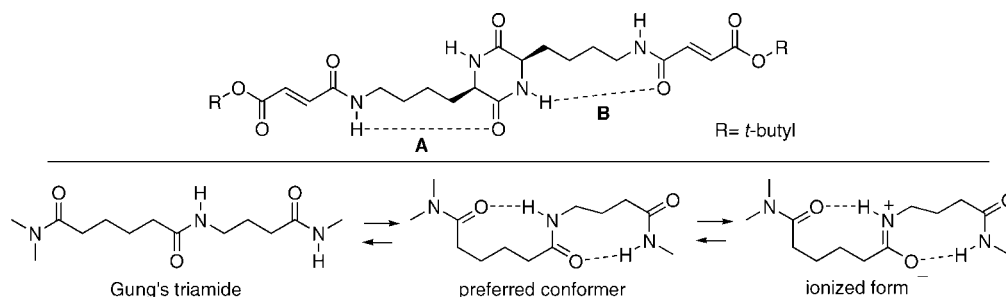


Figure 2. “Cooperative” hydrogen bond in **9a** involving both hydrogen-bonding types (**A** and **B**) and Gung's triamide.

show this property, and it is well-established that tertiary amides undergo cis–trans isomerism.¹⁹ At higher concentrations, only one NH population was observed, which may be due to the involvement of intermolecular hydrogen bonding^{2–4} or the fact that the NMR time scale (milliseconds) is slow and one is observing the time average of the NH population.¹³

Compound **9a** was synthesized to observe the hydrogen-bonding patterns of **2** in solution. As mentioned previously, it was not possible to directly study the diethyl ester of **1** (i.e., **2**) because it was insoluble in CDCl₃. Nevertheless, by changing the ethyl ester to a *tert*-butyl ester, we observed a modest increase in CDCl₃ solubility with **9a**. Although it was not freely soluble in CDCl₃, we were able to generate a 1 mM CDCl₃ solution of **9a**, which facilitated inspection by ¹H NMR and IR.

Two NH populations were observed in the ¹H NMR spectrum of **9a**. The high ppb/K values (i.e., 10.4 and 10.6) of these two NH signals show that each is involved in intramolecular hydrogen bond. As will be shown later, these were assigned to a “cooperative” hydrogen bond involving a type **A** hydrogen bond for one arm of the molecule and a type **B** hydrogen bond for the other arm (Figure 2). The large magnitudes observed with **9a** are consistent with those observed with the related acyclic triamides, which are also involved in cooperative hydrogen bonds (see Gung's triamide in Figure 2).¹³

The *N*-ethylated adduct **9b** was also studied by VT-NMR. *N*-Ethylation provided this freely soluble analogue of **2**, which was amenable to study by both ¹H NMR and IR. Four NH populations (**9b**-(1–4)) were observed in the ¹H NMR of **9b** in CDCl₃. **9b**-1 (10.6 ppb/K), **9b**-2 (6.5), and **9b**-3 (5.9) were assigned as intramolecularly bound NHs. The **9b**-4 NH population was tentatively assigned to solvent-exposed NH due to its lower temperature dependence (4.7 ppb/K). Again the rapid cis–trans isomerism associated with tertiary amides may explain the number of NH populations observed with these *N*-ethylated amide systems. Note: the 10.6 ppb/K NH population is likely due to type **B** hydrogen bonding, which is available in both systems **9a** and **9b**. Note: *trans*-

9c gave two NH populations like the cis isomer **9a**, albeit with lower temperature dependencies (6.3 and 4.8 ppb/K, respectively).

Compound **9d**, in which the diketopiperazine NH's are blocked by *N*-ethylation, showed one NH population in the VT-NMR study with a low temperature dependency (5.4 ppb/K). In this case, the cis–trans isomerism of the tertiary amide is not possible due to the constraints of the diketopiperazine ring. As a result, the isomeric possibilities are limited and one sees the expected singular NH population. These collective findings supported the premise of cooperative hydrogen bonding in **9a**.

Caveat. Since the NMR time scale is in milliseconds, it is slow compared to the IR time scale (nanoseconds) and may reveal simply the time-average of the NH signals. As such, one may observe a singular NH population in ¹H NMR but see two NH populations in the IR spectrum of the same solution.¹³ However, using both methods in tandem allowed for definitive conclusions to be reached.

FTIR Studies. The nanosecond time scale of infrared (IR) spectroscopy allows for direct inspection of each hydrogen-bonded species. [Note: hydrogen-bonded amide NHs usually occur near 3300–3400 cm^{−1} in the IR spectrum, and free NH's are typically >3400 cm^{−1}.]^{9,13–16} IR and NMR were used in tandem to delineate the type and nature of the H-bonding species involved. Acquiring IR spectra at 1, 10, and 100 mM of each compound in dry CHCl₃ revealed different IR patterns between 3100 and 3500 cm^{−1}. By obtaining this information on a series of model compounds (**3–8a**, **9a–d**), each of which has limited hydrogen-bonding possibilities, one can assign which specific intermolecular and intramolecular hydrogen bonds are preferred in **1**.

The structure of **1** lends itself to several possible hydrogen-bonding scenarios, and it is essential to identify which of these are involved in intra- and intermolecular bonds. As shown in Figure 1, several model compounds were chosen to assist with the IR peak assignments of the possible intramolecular hydrogen bonds in FDKP (**A–C**). Each derivative represents a modest alteration in the FDKP architecture and provided an IR frequency (or wavenumber expressed in cm^{−1}) associated with each type of intramolecular interaction. As reported previously, a 1 mM concentration is dilute enough to favor the formation of intramolecular hydrogen bonds. In contrast, the 100 mM solutions

(19) Portnova, S. L.; Bystrov, V. F.; Balashova, T. A.; Ivanov, V. T.; Ovchinnikov, Y. A. Cis-trans-isomerism of the peptide bond in *N*-methylated alanine dipeptides. *Russ. Chem. Bull.* **1970**, *19*, No. 4, 776–780.

Table 2. IR Frequency (cm^{-1}) of Free and Bonded NH in Compounds **3–9** in 1 mM Solution

compd	free NH		H-bonded NH			
3	3439 (48%)	3352 (8%)	3324 (10%)	3285 (32%)		3203 (2%)
4	3445 (61%)	3346 (16%)	3322 (23%)			
5	3450 (68%)	3341 (14%)	3332 (16%)		3230 (2%)	
6	3442 (37%)	3343 (5%)		3287 (55%)		3204 (3%)
7a	3440 (98%)	3357 (2%)		3280 (1%)		3199 (3%)
7b	3471 (2%)	3393 (48%)	3310 (30%)		3227 (18%)	3170 (2%)
8a	3449 (12%)	3390(61%), 3353 (7%)	3323 (3%)	3280 (5%)	3257 (10%)	3205 (2%)
9a	3456 (18%)	3389 (2%)	3302 (67%)			3180 (13%)
9b	3455 (1%)	3388(61%), 3357 (2%)	3319 (3%)	3257 (19%)	3238 (7%)	3209 (7%)
9c	3448 (21%)	3388 (6%)	3309 (44%)			3172 (29%)
9d	3441 (32%)		3318 (51%)	3236 (1%)		3150 (16%)

Table 3. IR Frequency (cm^{-1}) of Free and Bonded NH in Compounds **3–9** in 10 mM Solution

compd	free NH		H-bonded NH			
3	3439 (34%)	3352 (8%)		3285 (58%)		
4	3444 (57%)		3317 (43%)			
5	3450 (71%)		3332 (27%)			3222 (2%)
6	3441 (32%)	3350 (5%)		3288 (63%)		
7a	3440 (100%)					
8a	3441 (3%)	3390 (60%)	3320 (3%)		3256 (14%)	3224 (20%)
9b		3390 (58%)	3314 (1%)		3241 (27%)	3223 (14%)
9d	3443 (33%)		3318 (67%)			

are at a concentration which facilitates intermolecular contacts.^{9,13–16}

As shown in Figure 1, three types of intramolecular hydrogen bonding (designated as **A**, **B**, and **C**) are possible for **1** and its ethyl ester **2**. Clearly, there are more available, but we focused on these three because dealing with the free acid form **1** introduced another H bond donor (COOH), which would make the interpretation more complex, and we were also constrained by the poor solubility of both **1** and **2**. The esters were a reasonable tradeoff in order to investigate these molecular frameworks. *In addition, the IR data suggested that the carbonyl of the fumaryl ester group was not involved in the intramolecular hydrogen bond scenarios of these materials (see the Supporting Information).*

As shown in Tables 2–4, free amide NH absorption bands consistently appeared at $\sim 3445 \text{ cm}^{-1}$ for virtually all of the model compounds studied, which is consistent with that observed by other researchers.¹³ The percent free NH at 100 mM should be lower than that at 1 mM because the free NH can bond to other molecules at the higher concentration.

The % NH populations listed in Tables 2–4 provide a clear story of the NH-population preferences. Most of the models tested at 1 mM had a detectable amount of free NH population (i.e., unbound or solvent exposed NH), which varied depending upon the molecular architecture (see free NH column in Tables 2–4). Since the free NH population was ubiquitous, the following discussion will focus on the hydrogen bound species involved (which appear $< 3400 \text{ cm}^{-1}$ in the IR spectrum). The reader is referred to Tables 2–4 to observe the free NH population percentages. In general, the percentages are estimates of the area under the

Table 4. IR Frequency (cm^{-1}) of Free and Bonded NH in Compounds **3–9** in 100 mM

compd	free NH		H-bonded NH			
3	3439 (19%)	3378 (5%)		3292 (76%)		
4	3445 (32%)		3311 (68%)			
5	3449 (57%)		3337 (43%)			
6	3440 (16%)	3373 (7%)		3290 (77%)		
7a	3440 (58%)	3378 (27%)	3328 (15%)			
8a		3390 (38%)			3217 (62%)	
9b		3391 (37%)			3219 (63%)	
9d	3443 (19%)			3314 (81%)		

curves observed in the IR spectra in dry CHCl_3 . Some models could not be studied at higher concentrations due to solubility constraints.

Discussion

Compound **3** exclusively shows 9-membered hydrogen bonding **A** (Figure 1), and its IR spectrum shows that 48% of the NH population is the free NH (3439 cm^{-1}), whereas 52% is involved in forming intramolecular hydrogen bonds (1 mM **3** in CHCl_3). There were at least four different NH populations observed with only one major NH band predominating at 3285 cm^{-1} (32%), which was assigned to the 9-membered hydrogen bond **A**. The other IR bands were all $\leq 10\%$.

Compounds **4–6**, by design, differentiate between the two 10-membered hydrogen-bonding patterns (**B** and **C**). Compound **5** shows a unique H-bond absorbance at 3332 cm^{-1} .

This wavenumber was assigned to the 10-membered hydrogen bond **B** and not type **C**. In contrast, diamide **6** has a strong absorption band at 3287 cm^{-1} , which was assigned to a type **C** hydrogen bond. Both systems **5** and **6** have another weak band at 3341 and 3343 cm^{-1} , respectively, which is likely an artifact due to the high dilution. This artifact signal is not observed at the higher concentrations (10 and 100 mM), whereas the others are very apparent in the 10 mM and 100 mM samples (Tables 3 and 4).

We conclude that in the acyclic models the hydrogen bonds of types **A**, **B**, and **C** are at 3285 , 3332 , and 3287 cm^{-1} , respectively. Ironically, the nine membered type **A** (3285 cm^{-1}) observed in **3** comes very close to the wavenumber assigned to **C** (3287 cm^{-1}). In this regard, it may be difficult to distinguish between these two hydrogen bond types. This issue was addressed via molecular modeling studies, which demonstrated that **A** is significantly more stable than **C** due to geometric constraints (see the Molecular Modeling section).

Inspection of the parent system **4**, where both scenarios (**B** and **C**) are available, could now be interpreted. Diamide **4** gave an NH IR band near 3322 cm^{-1} , which is more consistent with model **5** (i.e., type **B**) than model **6** (type **C**). Moreover, this observation is perfectly consistent with the earlier NMR findings, where the magnitude of the ppb/K dependence was nearly identical for **4** and **5** (Table 1). In short, given the choice, this generic diamide scaffold preferred to adopt the 10-membered hydrogen bond type **B** (rather than **C**).

IR absorbance bands are broad and represent continuums of NH bonding environments. A particular interaction is assigned to a particular wavenumber (cm^{-1}). This wavenumber is the frequency of maximal absorbance of each IR absorption band. In compound **7a**, 98% of the NH population by IR analysis is “free” NH at 3440 cm^{-1} . This is again consistent with our NMR findings (**7a**: 2.8 ppb/K), which support the fact that the ester carbonyl is not playing a role in the hydrogen bonding of the fumaramide NH (see also Figure 1: **7a**). In this regard, the ester strategy was a good choice to pursue these analyses, and the seven-membered hydrogen bond shown in Figure 1 was not significant. This observation considerably simplified the IR analysis as one could disregard interactions between the fumaramide NH and the appended ester. Note: **7a** was not soluble above 1 mM in chloroform.

By design, the *N*-ethylated derivative **8a** (*S,S*-isomer) has only the 10-membered hydrogen bond (type **B**) available for its intramolecular contact. As shown in Table 2, model **8a** has 12% of the NH population as free NH, and the rest is involved in intramolecular hydrogen bonding. There are four populations (>5%) of bonded NH's (which are easier to see at 10 mM, Table 3). The IR data of compound **8a** shows a strong peak for the 10-membered hydrogen bond (**B**) at 3390 cm^{-1} (61%), which is different from what was observed for **B** in compound **5** (3332 cm^{-1}). This 58 cm^{-1} difference could stem from the architectural constraints imparted by the rigid diketopiperazine platform versus the flexible acyclic

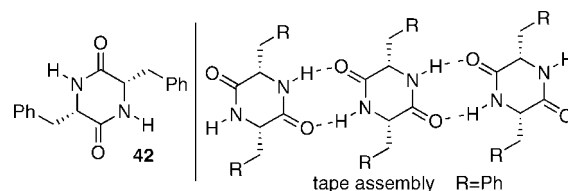


Figure 3. Compound **42** and its putative self-assembled tape.³

system in models **4–6**. Nevertheless, the 3390 cm^{-1} is much closer to 3332 cm^{-1} (**B**) than the 3287 cm^{-1} frequency associated with **C** (over 100 cm^{-1} away).

Control experiments with saturated solutions of the diketopiperazine of L-Phe, **42**,²⁰ revealed a similar band at 3390 cm^{-1} , which is consistent with the hydrogen-bonded diketopiperazine NH. This control compound was virtually insoluble in CDCl_3 and at best formed a gelatinous slurry. In this regard, we assigned this wavenumber to an intermolecular contact (Figure 3).³

Unfortunately, the ethyl ester **2** was not soluble in CDCl_3 . Therefore, *tert*-butyl ester **9a** was synthesized in order to see these interactions within the parent molecule **2**. The replacement of the ethyl group with the *tert*-butyl group indeed facilitated the generation of a 1 mM solution of **9a**. However, **9a** was not soluble in CDCl_3 at concentrations above 1 mM. The data acquired at 1 mM **9a** is shown in Table 2. Compound **9a** gave 18% free NH population and the rest, 82%, was involved in intramolecular hydrogen bonds. The major intramolecularly bound NH bands observed for **9a** were at 3302 cm^{-1} (67%) and 3180 cm^{-1} (13%), respectively. Note: 3302 cm^{-1} is a unique wavenumber and was assigned to a cooperative hydrogen bond as shown in Figure 2 (see the Molecular Modeling section).

In order to further probe these interactions, we synthesized (*N*-ethyl)-*tert*-butyl ester **9b**. Indeed, **9b** was similar to the (*N*-ethyl)-ethyl ester **8a**, and both were significantly more soluble than **2** and **9a**. Recall that the NMR data revealed four NH populations for both **8a** and **9b**, respectively (Table 1). In terms of the IR data at 1 mM **9b**, only 1% of the NH population is solvent-exposed, and the molecule is essentially intramolecularly hydrogen bound. While at least six NH populations were detected, the major intramolecularly bound NH bands were at 3388 cm^{-1} (61%) and 3257 cm^{-1} (19%) (at 1 mM **9b** in CDCl_3). At higher concentrations, there were essentially two major bands [at 3390 and a broadband centered at 3241 cm^{-1} (for 10 mM **9b**) and at 3391 and 3219 cm^{-1} for 100 mM **9b**]. The band at 3390 cm^{-1} was assigned to a hydrogen-bonded diketopiperazine NH involved in a type **B** hydrogen bond. Note: a “tape motif” similar to that depicted in Figure 3 was ruled out for **9b** due to the failed assembly experiments with its free acid form, **8b**, described later in this report.

As shown in Table 2, the trans isomer **9c** gave an IR spectrum that was similar to that of the cis isomer **9a** (at 1

(20) Jung, M. E.; Rohloff, J. C. Organic Chemistry of L-Tyrosine.1. General Synthesis of Chiral Piperazines from Amino Acids. *J. Org. Chem.* **1985**, 50, 4909–4913.

mM). This implied that both isomers were able to adopt similar hydrogen-bonding motifs. This insight was very useful in discrediting an interchain model, which was only possible via the *cis* framework (see the Molecular Modeling section).

Comparisons between compounds **8a** and **9a–d** provided valuable insights. Clearly, *N*-ethylation of the fumaramide NH (i.e., **8a** and **9b**) gave a different hydrogen-bound NH population (3390 and 3257 cm⁻¹) than when this NH is available (e.g., **9a** gave 3302 cm⁻¹ and 3180 cm⁻¹). In the case of the *N*-ethylated diketopiperazine (**9d**), 3390 cm⁻¹ was not observed and allowed for the confirmed assignment of 3390 cm⁻¹ as the diketopiperazine H-bound NH population. A band was observed with **9d** at 3318 cm⁻¹, which was different from the frequency assigned to cooperative hydrogen bonding (3302 cm⁻¹) observed in **9a** and could be due to either **A** or **C** type hydrogen bonding. Indeed, the acyclic models, the diketopiperazine control, and models **8a** and **9b** all suggested that a hydrogen bond of type **B** was prevalent when the diketopiperazine NH is available. Moreover, the one-arm control **7b** gave the same NH population (3393 cm⁻¹, 48%), which is also consistent with type **B** hydrogen bonding.

In this regard, why are **9a** and **9c** so different from the other diketopiperazine models? The answer came from our molecular modeling investigations of these systems. As shown in Figure 2, **9a** is involved in a cooperative hydrogen bond, which involves *both* arms of the molecule to form both type **B** and type **A** hydrogen bonds. The reason the IR bands for **9a** are unique is because with both fumaramides available, **9a** can create a cooperative hydrogen bond involving one of the diketopiperazine amide groups and both of the side chains (see Figure 1, **9a**). Since the cooperative hydrogen bond involves both the carbonyl and the NH of the diketopiperazine amide group, the frequency associated with the type **B** hydrogen bond in **9a** is shifted to lower frequency (3302 cm⁻¹). Indeed, this cooperativity has been shown to be a stabilizing feature in other triamide systems (with similar spacings) by Gung et al.¹³ and is also accessible to the *trans* isomer **9c** (Table 2).

Molecular Modeling. In order to evaluate the preferred hydrogen-bonding motifs present in **2**, molecular modeling experiments were performed. To winnow out the most stable conformers, two procedures were employed: the systematic approach and the Monte Carlo method. Past experience has demonstrated that the odds of capturing the most stable conformer were improved if these two entirely different methodologies were used.²⁰ The approach started with the “one-armed” control **7b**.

Each model was built in successive steps by first performing MMFF (molecular mechanics) and PM3 semiempirical (quantum mechanical) calculations on 3,6-dimethyldiketopiperazine to give one conformer. The methyl groups were replaced with the appropriate side chains of **7b**. The different hydrogen bond types (**A–C**) were mechanically formed, followed by geometry optimization using increasingly more accurate methodologies: MMFF, PM3, STO-3G, and 3-21G(d). The final structure is the one that was geometry optimized

using the Hartree–Fock method with the 3-21G(d) basis set, and then the energy was much more accurately computed using density functional theory, B3LYP, i.e., structure via HF/3-21G(d) and energy via SP/DFT/B3LYP/6-31G(d). This is a combination of computations that is commonly used in conformer searching and gave a final structure (with associated energy).²¹

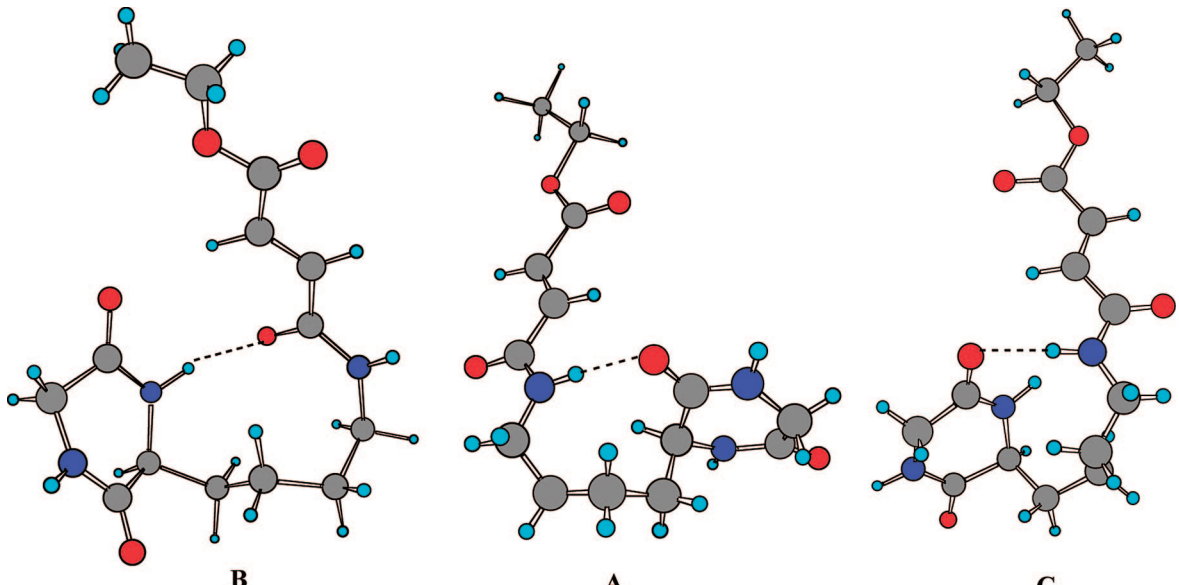
The results for the lowest energy conformer containing one of the three hydrogen bond types are shown in Table 5. In model **7b**, type **B** hydrogen bonding was 2.88 and 4.86 kcal/mol lower in energy than **A** and **C**, respectively. An attempt to simultaneously form both type **A** and **B** motifs in **7b**, i.e., a cooperative hydrogen bond on one arm, resulted in a structure that was 23 kcal/mol higher than **B** alone. Therefore, we ruled out the possibility of cooperative hydrogen bond using one arm only.

In a similar manner, model **9a** (*S,S* isomer) was constructed and geometry optimized. Due to computational time constraints, the *Nε*-fumaramide group was replaced by a *Nε*-formamide group to simplify the calculations. Once optimized at the 3-21G level, the remaining fumaramide motif was then added and optimized at the 6-31G(d) level. As shown in Table 6, the cooperative hydrogen bond (**AB**) was preferred.

Due to the significant energy differences between the calculated structures, the cooperative hydrogen-bonding motif (**AB**) was most consistent with our experimental data. According to Gung, a cooperative hydrogen bond should be nearly linear for optimal hydrogen bond strength.¹³ The two respective (O–H–N) bond angles in the *cis* **AB** model shown in Table 6 were 167.5° and 155.4°, respectively. As shown in Table 6, the **AB** conformer orients the appended fumarate arms in a nearly 90° orientation with respect to each other. This orients the complementary hydrogen bond donors (amide NH and COOH) and acceptors (amide and carboxylic acid carbonyls) along discreet axes for intermolecular hydrogen bonding. Interestingly, this motif resembles the classic β hairpin (type II). Note: this assignment is based on the orientation of the functional groups and direction of the amide bonds in the backbone. Although the H-bonding pattern is typical, a more interesting nuance is that these types of turns (within proteins) are usually the regions of interaction with protein receptors.²²

The interchain 1 model in Table 6 was ruled out because the *trans* isomer **9c** had an IR spectrum at 1 mM nearly identical to that of the *cis* isomer, (*R,R*)-**9a**, and had a similar stability trend in terms of the **AB** vs **AA** and **BB** models

- (21) Breitbeil, F., III; Kaur, N.; Delcros, J.-G.; Martin, B.; Abboud, K. A.; Phanstiel, O., IV. Modeling the Preferred Shapes of Polyamine Transporter Ligands and Dihydromotuporamine-C Mimics: Shovel versus Hoe. *J. Med. Chem.* **2006**, *49*, 2407–2416.
- (22) Wheat, W.; Fitzsimmons, D.; Lennox, H.; Krautkramer, S. R.; Gentile, L. N.; McIntosh, L. P.; Hagman, J. The Highly Conserved beta-Hairpin of the Paired DNA-Binding Domain Is Required for Assembly of Pax-Ets Ternary Complexes. *Mol. Cell. Biol.* **1999**, *19*, 2231–2241.

Table 5. Relative Energies of Hydrogen bonds A–C in **7b**


H-bond type	rel energy (kcal/mol)	H-bond distance (Å)
B	0.00	2.79
A	2.88	2.86
C	4.86	2.79

(Table 7). In addition, the VTNMR experiments with *trans*-**9c** revealed only two NH populations, which were similar to the two observed with the *cis* isomer **9a**, albeit with lower temperature dependencies (**9a**: 10.6 and 10.4 ppb/K; **9c**: 6.3 and 4.8 ppb/K, respectively). This implied that these isomers likely form similar hydrogen bond motifs. The lower temperature dependencies observed with **9c** could be due to the fact that the AB conformer of *trans*- is higher in energy (5.78 kcal/mol) than the AB conformer of its (*S,S*) *cis* isomer. This may be due to weaker hydrogen bonds in **9c**. The “interchain 1” motif cannot be formed by the *trans* isomer (without the introduction of significant torsional strain) because the arms are oriented on opposite sides of the diketopiperazine ring.

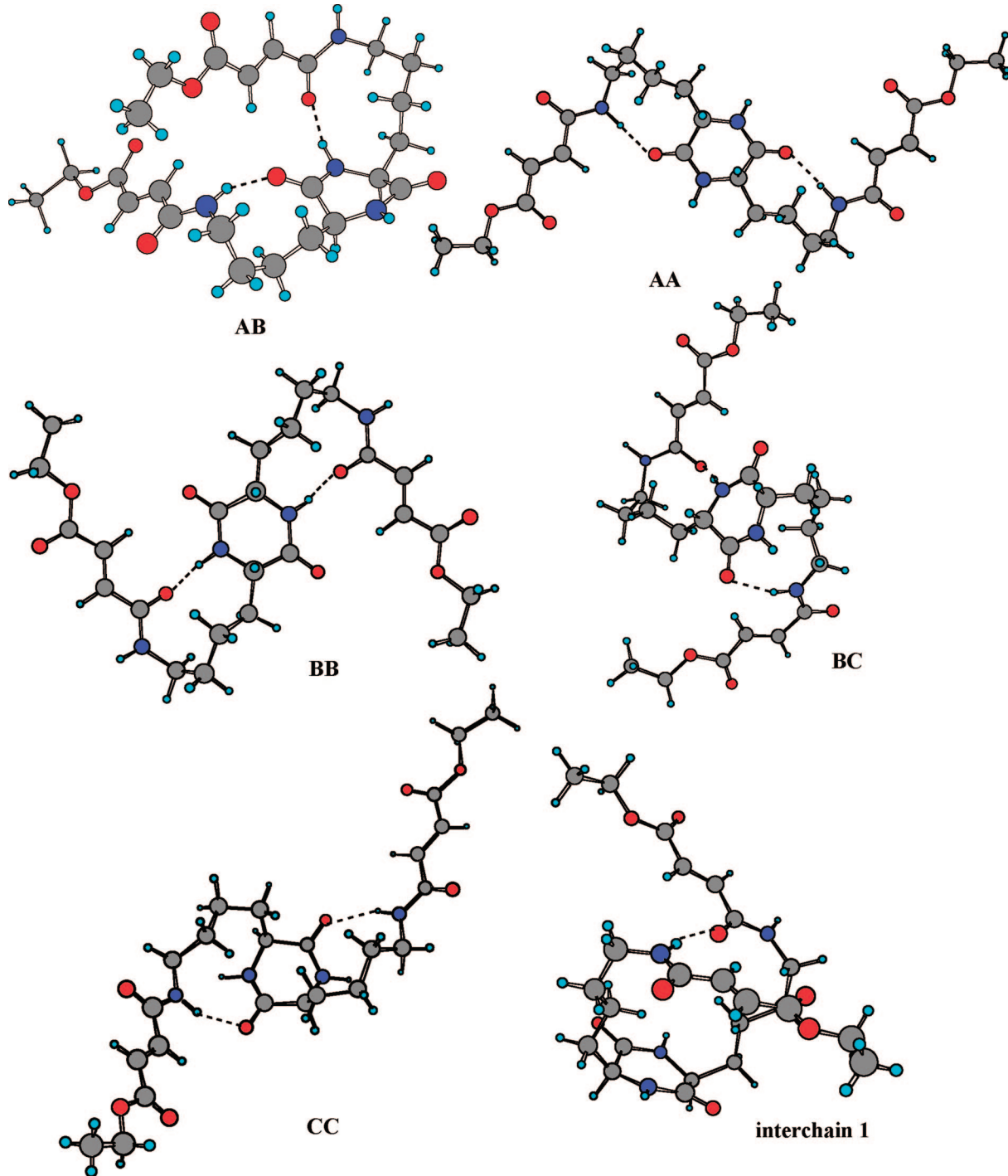
Possible Caveat. We speculated that although both **42** and **9b** contain the same 3390 cm^{−1} IR band, this frequency may simply indicate that the diketopiperazine amide is involved in a hydrogen bond and does not identify its complementary bonding partner *per se*. Indeed, due to the geometries of the large 10-membered (type **B**) and 9-membered (type **A**) rings, the frequency associated with an intramolecular hydrogen bond and an intermolecular structure (the “tape” interaction) may be indistinguishable in the IR spectrum (Figure 4).

Testable Hypothesis. In order to test this hypothesis, models **1b** (4.2 g) and **8b** (3.2 g) were synthesized on a larger scale. After careful evaluation, the *cis* isomer **1b** was able to form microparticles, whereas the *N*-ethylated analogue **8b** did not. This confirmed that, indeed, the fumaramide NH was involved in the self-assembly of **1**.

The negative assembly result found with **8b** was also very insightful. Since the diketopiperazine amide groups were available for intermolecular contacts in **8b**, it could have self-assembled via the tape arrangement shown in Figure 3 using amide-to-amide intermolecular contacts (e.g., the “tape” in Figure 4). However, since **8b** did not self-assemble, the tape motif was ruled out as a probable self-assembly mechanism for these constructs under these assembly conditions (see the Experimental Section).

Summary

All of our observations suggest that a hydrogen bond of type **B** is preferred by the scaffold of **2** (and presumably **1**) for the following reasons. First, given the choice in compound **4**, the 10-membered hydrogen bond **B** was the preferred interaction. Second, once **B** is formed, it would activate the associated diketopiperazine carbonyl for docking to an adjacent hydrogen-bond donor.¹³ The appended fumaramide NH of the other arm could act as an intramolecular donor to form the **A**-type hydrogen bond. The fact that the solubility of **2** dramatically changes when this fumaramide position is *N*-ethylated (i.e., blocked as in the case with **8a** and **9b**) supports this premise. Third, the IR absorbance band at 3390 cm^{−1} is a major contributor to the IR population even at higher concentrations (i.e., 100 mM **9b**). This suggests that this intramolecular interaction is not only stable, but preferred across a wide concentration range. Fourth, molecular modeling suggested that the cooperative hydrogen bond (**AB** type, Figure 1 for **9a**) is most energetically favorable. Fifth, a derivative wherein this interaction was

Table 6. Relative Energies of A–C Bonding Motifs in a Double-Armed Model of (S,S)-9a

H-bond type	rel energy (kcal/mol)
AB	0.00
interchain 1 ^a	0.76
AA	2.39
BB	3.13
BC	9.80
CC	15.12
AC ^b	NA

^a Contains a hydrogen bond between the fumaramide groups on opposite arms. ^b The AC hydrogen-bonded model could be constructed mechanically using the constraints and freeze options of SpartanPro, but when geometry optimizing, the algorithm overrode the hydrogen bonding due to significant steric and torsional interactions. The A type hydrogen bond survived, while the C type was broken.

Table 7. Molecular Modeling Results for the Three Hydrogen-Bonding Scenarios of the *trans*-(*R,S*)-**9c**

H-bond type	rel energy (kcal/mol)
AB	0.00
AA	2.21
BB	2.80

blocked (**8b**) did not undergo the assembly process. Collectively, these data suggest a cooperative hydrogen-bonding scenario as the key driver of the self-assembly of **1**. A cooperative hydrogen bond (AB type shown in Figure 1) within the molecular framework of **1** initiates its self-assembly by orienting the amide and carboxylic acid motifs for intermolecular hydrogen bonding via noncovalent interactions.^{11,12}

Experimental Section

Materials. Silica gel (32–63 μm) and chemical reagents and control diketopiperazine **42** were purchased from commercial sources and used without further purification. All solvents were distilled prior to use. ^1H and ^{13}C NMR spectra were recorded at 300 and 75 MHz, respectively. TLC solvent systems are based on volume percent, and NH_4OH refers to concentrated aqueous NH_4OH . Samples for elemental analyses were sent to Atlantic Microlabs (Norcross, GA) and for high-resolution mass spectrometry were sent to the University of Florida Mass Spectrometry facility. The fumarate derivatives **10** and **24a** and diketopiperazines **25b** and **35** were generously provided by MannKind Corp. (Danbury, CT).

Self-Assembly Test. Each model (**1b** and **8b**) was dissolved in aqueous NaOH to form a 2.5 wt % aqueous solution. This solution was then added to a stirred solution of acetic acid (10.5 wt %) at 16 $^\circ\text{C}$. Microparticles of **1b** formed instantly and generated a suspension, which was filtered. Compound **8b** did not precipitate, and no microparticles were observed.

Large-Scale Process. Using the Dual-feed Sonolator, equal masses of 10.5 wt % acetic acid and 2.5 wt % aqueous solutions of the respective model (**1b** or **8b**) at pH 9 at 16 $^\circ\text{C} \pm 2$ $^\circ\text{C}$ (Tables 1 and 2) were fed at 2000 psi through a 0.001 in.² orifice. The precipitate observed with **1b** was collected in a DI water reservoir of equal mass and

temperature. The precipitate was concentrated and washed by tangential flow filtration. The suspension was finally concentrated to 10% solids based on the initial mass of **1b**.

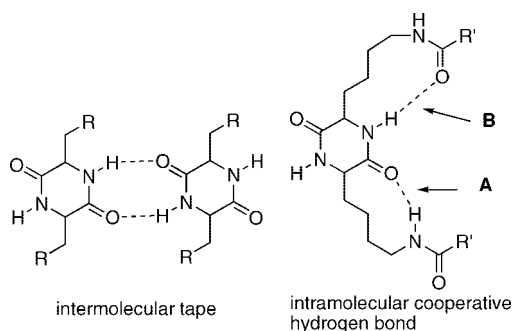
cis-3-(4-{5-[4-(3-Carboxyacryloylamino)butyl]-3,6-dioxopiperazin-2-yl}butylcarbamoyl)acrylic Acid (1b**).** A 5.5 g portion of *cis*-di-*tert*-butyl ester **9a** was stirred in 50% TFA/ CH_2Cl_2 for 1 h at rt. After the consumption of **9a** was monitored by TLC in 9% MeOH/1% $\text{NH}_4\text{OH}/\text{CH}_2\text{Cl}_2$ ($R_f = 0.4$), the solvents were removed under vacuum. The solid residue obtained was washed with MeOH and dried under vacuum to obtain white solid **1b** in 94% yield: ^1H NMR ($(\text{CD}_3)_2\text{SO}$) δ 8.45 (t, 2H, NH), 8.10 (br s, 2H, NH), 6.90 (d, 2H, CH), 6.48 (d, 2H, CH), 3.78 (t, 2H, CH), 3.13 (q, 4H, NCH_2), 1.66 (q, 4H, CH_2), 1.42 (m, 4H, CH_2), 1.33 (m, 4H, CH_2); ^{13}C NMR ($(\text{CD}_3)_2\text{SO}$) δ 167.6, 166.3, 162.7, 137.0, 129.2, 53.9, 32.8, 28.6, 21.9. *R,R* isomer: $[\alpha]^{25}_{546} +18$ (*c* 1, DMSO).

FDKP-OEt, 2. The respective *cis* and *trans* isomers of FDKP-OEt were received from MannKind Corp. Note: neither of these was soluble in CDCl_3 .

Cis isomer of **2**: ^1H NMR ($\text{DMSO}-d_6$) δ 8.49 (t, 2H, NH), 8.10 (br s, 2H, NH), 6.97 (d, 2H, CH), 6.53 (d, 2H, CH), 4.16 (q, 4H, OCH_2), 3.79 (t, 2H, $\alpha\text{-CH}$), 3.15 (q, 4H, NCH_2), 1.64 (quin, 4H, CH_2), 1.42 (m, 4H, CH_2), 1.34–1.21 (m, 7H, CH_2 and CH_3). *Trans* isomer of **2**: ^1H NMR ($\text{DMSO}-d_6$): δ 8.50 (t, 2H, NH), 8.10 (br s, 2H, NH), 6.98 (d, 2H, CH), 6.53 (d, 2H, CH), 4.17 (q, 4H, OCH_2), 3.80 (t, 2H, $\alpha\text{-CH}$), 3.15 (q, 4H, NCH_2), 1.68 (quin, 4H, CH_2), 1.41 (m, 4H, CH_2), 1.33–1.21 (m, 7H, CH_2 and CH_3); $[\alpha]^{25}_{546}$ 0 (*c* 1, DMSO).

3-(5-Diethylcarbamoylpentylcarbamoyl)acrylic Acid Ethyl Ester (3**).** To the stirring solution of acid **12** (250 mg, 0.97 mmol) and 1*H*-benzotriazol-1-yloxytris(dimethylamino)phosphonium hexafluorophosphate (BOP, 430 mg, 0.97 mmol, in dry CH_2Cl_2 (10 mL)) was added diethylamine (250 mg, 3.42 mmol) at 25 $^\circ\text{C}$. The reaction mixture was allowed to stir overnight under a N_2 atmosphere. After the consumption of **12** was checked by TLC (R_f 0.3 in 5% MeOH/ CH_2Cl_2), the solution was washed three times with aqueous sodium carbonate. The organic layer was separated, dried with anhydrous Na_2SO_4 , filtered, and concentrated under vacuum to give a pale yellow oil, which was further purified by column chromatography using 3% MeOH/ CH_2Cl_2 to give **3** in 84% yield: R_f 0.3, 3% MeOH/ CH_2Cl_2 ; ^1H NMR (CDCl_3) δ 8.03 (br s, 1H, NH), 7.07, 6.80 (q, 2H, CH), 4.23 (q, 2H, OCH_2), 3.31–3.41 (m, 6H, NCH_2), 2.33 (t, 2H, COCH_2), 1.66 (q, 2H, CH_2), 1.60 (q, 2H, CH_2), 1.40 (q, 2H, CH_2), 1.31 (t, 3H, CH_3), 1.18 (t, 3H, CH_3), 1.13 (t, 3H, CH_3); ^{13}C NMR (CDCl_3) δ 171.9, 165.6, 163.8, 137.1, 129.2, 60.7, 41.9, 40.0, 39.3, 32.6, 28.8, 26.4, 24.6, 14.1, 14.0, 12.9; HRMS (FAB) m/z calcd for $\text{C}_{16}\text{H}_{28}\text{N}_2\text{O}_4$ ($M + \text{H}$)⁺ 313.2122, found 313.2108.

3-(7-Oxoocetylcarbamoyl)acrylic Acid Ethyl Ester (4**).** Anhydrous Na_2CO_3 (68 mg, 0.64 mmol) was added to the stirring solution of compound **16** (116 mg) dissolved in TEA (5 mL) and dry THF (10 mL). A solution of **10** (169.6 mg, 0.64 mmol) in dry THF (10 mL) was added dropwise to the

**Figure 4.** Intermolecular tape versus the intramolecular cooperative hydrogen bond type A/B.

reaction mixture at 0 °C. The reaction mixture was allowed to stir overnight. The mixture was then filtered and concentrated. The residue was dissolved in CH₂Cl₂ (10 mL) and washed two times with saturated aq Na₂CO₃. The organic layer was separated, dried with anhydrous Na₂SO₄, filtered, and concentrated. The yellow residue was purified by column chromatography (0.3% NH₄OH/6% MeOH/CH₂Cl₂) to give pure **4** in 56% yield: *R_f* = 0.33; ¹H NMR (CDCl₃) δ 6.93 (d, 1H, CH), 6.78 (d, 1H, CH), 6.49 (s, 1H, NH), 5.78 (s, 1H, NH), 4.24 (q, 2H, OCH₂), 3.35 (q, 2H, NCH₂), 3.27 (q, 2H, NCH₂), 1.99 (s, 3H, CH₃), 1.57 (m, 4H, CH₂), 1.32 (m, 5H, CH₃, CH₂); ¹³C NMR (CDCl₃) δ 164.1, 136.7, 130.4, 109.7, 77.7, 77.3, 76.9, 61.5, 39.8, 39.3, 29.4, 28.8, 23.8, 23.7, 14.6; HRMS (FAB) *m/z* calcd for C₁₃H₂₂N₂O₄ (M + H)⁺ 271.1652, found 271.1645.

3-[(5-Acetylaminopentyl)ethylcarbamoyl]acrylic Acid Ethyl Ester (5). Acetyl chloride (78.5 mg, 1 mmol) was added at 10 °C to a vigorously stirred solution of **19** (72 mg, 0.20 mmol) dissolved in CH₂Cl₂ (10 mL) and saturated Na₂CO₃ aqueous solution (10 mL). The reaction mixture was allowed to stir for 5 h under a N₂ atmosphere. After the consumption of **19** was checked by TLC (*R_f* 0.28 in 1% NH₄OH/10% MeOH/CH₂Cl₂), the organic layer was separated, dried with anhydrous Na₂SO₄, filtered, and concentrated under vacuum to give an oil, which was further purified by column chromatography using 4% MeOH/CH₂Cl₂ to give **5** in 77% yield: *R_f* 0.32 in 4% MeOH/CH₂Cl₂; ¹H NMR (CDCl₃) δ 7.32 (m, 1H, CH), 6.79 (m, 1H, CH), 6.10, 5.84 (two br t, 2H, NH), 4.25 (q, 2H, OCH₂), 3.43 (q, 4H, NCH₂), 3.23 (q, 2H, NCH₂), 1.97 (t, 3H, CH₃), 1.56 (m, 4H, CH₂), 1.34, 1.22, 1.17 (2m, 8H, CH₃); ¹³C NMR (CDCl₃) δ 170.4, 170.4, 166.1, 165.9, 164.5, 164.0, 134.2, 134.0, 131.5, 131.3, 109.7, 77.8, 77.4, 76.9, 61.5, 48.0, 45.9, 43.2, 41.8, 39.7, 39.6, 29.7, 29.7, 29.1, 27.6, 24.3, 24.3, 23.6, 15.4, 14.6, 13.2; HRMS (FAB) *m/z* calcd for C₁₅H₂₆N₂O₄ (M + H)⁺ 299.1965, found 299.1956.

3-[(5-Acetyethylamino)pentylcarbamoyl]acrylic Acid Ethyl Ester (6). Compound **10** (90 mg, 0.34 mmol) in CH₂Cl₂ (10 mL) was added dropwise to the vigorously stirring mixture of **22b** (93 mg, 0.32 mmol) in CH₂Cl₂ (10 mL) and saturated Na₂CO₃ solution (10 mL) at 0 °C. The reaction mixture was stirred overnight. After the consumption of **22b** was checked, the organic layer was separated and concentrated under high vacuum. The residue obtained was redissolved in CH₂Cl₂ (20 mL) and washed two times with saturated aq Na₂CO₃. The organic layer was dried with anhydrous sodium sulfate and concentrated to give a residue, which was further purified by column chromatography (4% MeOH/CH₂Cl₂) to give pure **6** (60%): *R_f* = 0.31; ¹H NMR (CDCl₃) δ 6.97 (d, 1H, CH), 6.79 (d, 1H, CH), 4.22 (q, 2H, OCH₂), 3.32 (q, 6H, NCH₂), 2.10 (t, 3H, CH₃), 1.58 (m, 4H, CH₂), 1.35 (t, 2H, CH₃), 1.18 (t, 2H, CH₂), 1.10 (t, 1H, CH₂); ¹³C NMR (CDCl₃) δ 170.7, 170.0, 165.9, 165.8, 164.1, 164.0, 137.2, 136.8, 130.3, 129.8, 61.4, 61.3, 48.6, 44.5, 43.4, 40.8, 40.0, 39.9, 29.6, 29.0, 28.3, 27.5, 24.6, 24.0, 21.9, 21.8, 14.5, 14.4, 13.4; HRMS (FAB) *m/z* calcd for C₁₅H₂₆N₂O₄ (M + H)⁺ 299.1965, found 299.1955.

3-Butylcarbamoylacrylic Acid Ethyl Ester (7a). A solution of **10** (300 mg, 1.70 mmol) in dry THF (15 mL) was added dropwise to a stirring solution of the *n*-butylamine (124 mg, 1.5 mmol) and anhydrous Na₂CO₃ (180 mg, 1.2 mmol) in dry THF (10 mL) at 0 °C over a period of 1 h under an N₂ atmosphere. After the addition was complete, the reaction mixture was stirred overnight. After the consumption of **10** was checked by TLC (*R_f* of **10**: 0.35 in 60% CH₂Cl₂/hexane), the solution was filtered and the solvent was removed under vacuum. The residue was dissolved in CH₂Cl₂ (40 mL) and washed three times with aqueous sodium carbonate. The organic layer was separated, dried with anhydrous Na₂SO₄, filtered, and concentrated under vacuum to give a yellow solid **7a**, which was further purified by column chromatography using 1% MeOH/CH₂Cl₂ to give **7a** in 70% yield: *R_f* 0.3, 1% MeOH/CH₂Cl₂; ¹H NMR (CDCl₃) δ 7.37 (br s, 1H, NH), 7.07 (d, 1H, CH), 6.79 (d, 1H, CH), 4.26 (q, 2H, OCH₂), 3.35 (q, 2H, NCH₂), 1.54 (q, 2H, CH₂), 1.34 (q, 2H, CH₂), 1.26 (t, 3H, CH₃), 0.93 (t, 3H, CH₃); ¹³C NMR (CDCl₃) δ 165.7, 163.8, 137.0, 129.6, 61.1, 39.7, 31.4, 20.2, 14.2, 13.8; HRMS (FAB) *m/z* calcd for C₁₀H₁₇NO₃ (M + H)⁺ 200.1281, found 200.1276.

3-[4-(3,6-Dioxopiperazin-2-yl)butylcarbamoyl]acrylic Acid *tert*-Butyl Ester (7b). A solution of **34** (1.14 g, 4.65 mmol) in THF (40 mL) was added dropwise to a stirring solution of the acetic acid salt of diketopiperazine amine **23c** (3.4 g, 7.87 mmol) in aqueous Na₂CO₃ solution (5.0 g, 47.2 mmol) in THF (10 mL) at 0 °C over a period of 20 min under an N₂ atmosphere. After the addition was complete, the reaction mixture was allowed to stir at rt overnight. THF was evaporated under vacuum, and CH₂Cl₂ (250 mL) was added to the aqueous layer. The aqueous layer was extracted three times with CH₂Cl₂. The organic layers were combined, dried over Na₂SO₄, filtered, and concentrated under vacuum. Compound **7b** was purified by column chromatography using 6% MeOH/CH₂Cl₂ in 58% yield: *R_f* 0.3; ¹H NMR ((CD₃)₂SO) δ 8.59 (t, 1H, NH), 8.27 (s, 1H, NH), 8.09 (s, 1H, NH), 6.97 (d, 1H, CH), 6.53 (d, 1H, CH), 3.91–3.71 (m, 3H, CH₂, CH), 3.23 (q, 2H, NCH₂), 1.76 (m, 2H, CH₂), 1.82 (m, 2H, CH₂), 1.54 (m, 11H, CH₂, CH₃), 1.44 (m, 2H, CH₂); ¹³C NMR ((CD₃)₂SO) δ 167.6, 165.8, 164.0, 162.4, 136.6, 129.6, 80.8, 54.0, 44.3, 32.5, 28.6, 27.7, 21.7; HRMS (FAB) *m/z* calcd for C₁₆H₂₅N₃O₅ (M + Na)⁺ 362.1686, found 362.1646.

***cis*-3-[[4-(5-{4-[(3-Ethoxycarbonylacryloyl)ethylamino]-butyl}-3,6-dioxopiperazin-2-yl)butyl]ethylcarbamoyl]-acrylic Acid Ethyl Ester (8a).** A solution of **10** (95 mg, 0.36 mmol) in dry THF (10 mL) was added dropwise to a stirring solution of the acetic acid salt of *N*-ethylamine **28** (85 mg, 0.20 mmol), triethylamine (60 mg, 0.59 mmol), and anhydrous Na₂CO₃ (46 mg, 0.43 mmol) in dry THF (10 mL) at rt over a period of 1 h under an N₂ atmosphere. After the addition was complete, the reaction mixture was stirred overnight. After the consumption of **10** was checked by TLC (*R_f* of **10**: 0.35 in 60% CH₂Cl₂/hexane), the solution was filtered and the solvent was removed. The residue was dissolved in CH₂Cl₂ (40 mL) and washed three times with aqueous sodium carbonate. The organic layer was separated,

dried with anhydrous Na_2SO_4 , filtered, and concentrated under vacuum to give a residue, which was further purified by column chromatography using 5% MeOH/ CH_2Cl_2 to give **8a** as a white solid in 54% yield: R_f 0.3, 5% MeOH/ CH_2Cl_2 ; ^1H NMR (CDCl_3) δ 7.35 (m, 3H, CH, NH), 6.81 (m, 1H, CH), 4.26 (q, 4H, OCH_2), 3.98 (br t, 2H, CH), 3.42 (m, 8H, NCH_2), 1.98 (m, 2H, CH_2), 1.83 (q, 2H, CH_2), 1.63 (m, 4H, CH_2), 1.43 (m, 4H, CH_2), 1.32, 1.25, 1.17 (3t, 12H, CH_3); ^{13}C NMR (CDCl_3) δ 180.5, 168.9, 168.8, 168.4, 166.1, 165.9, 164.5, 164.5, 164.1, 134.1, 133.9, 133.8, 131.7, 131.6, 131.5, 131.4, 61.3, 54.9, 47.6, 45.7, 43.0, 41.6, 33.7, 33.5, 33.4, 29.4, 29.4, 27.4, 27.3, 22.3, 22.2, 22.1, 15.1, 14.3, 13.0; HRMS (FAB) m/z calcd for $\text{C}_{28}\text{H}_{44}\text{N}_4\text{O}_8$ ($\text{M} + \text{H}$) $^+$ 565.3232, found 565.3197.

3-[[4-(5-[4-[(3-Carboxyacryloyl)ethylamino]butyl]-3,6-dioxopiperazin-2-yl)butyl]ethylcarbamoyl]acrylic Acid (8b). The *N*-ethylated di-*tert*-butyl ester **9b** (4.5 g) was stirred in 50% TFA/ CH_2Cl_2 for 1 h at rt. After the consumption of **9b** was monitored by TLC in 7% MeOH/1% $\text{NH}_4\text{OH}/\text{CH}_2\text{Cl}_2$ (R_f = 0.4), solvents were removed under vacuum. The residue obtained was redissolved in CH_2Cl_2 and evaporated to get rid of TFA. The solid residue was dried under vacuum overnight to obtain white solid **8b** in 92% yield: ^1H NMR ($(\text{CD}_3)_2\text{SO}$) δ 8.11 (d, 2H, NH), 7.28 (d, 2H, CH), 6.51 (d, 2H, CH), 3.80 (br s, 2H, CH), 3.37 (m, 8H, NCH_2), 1.68 (m, 4H, CH_2), 1.48 (m, 4H, CH_2), 1.29 (m, 4H, CH_2), 1.08 (2t, 6H, CH_3); ^{13}C NMR ($(\text{CD}_3)_2\text{SO}/\text{CDCl}_3$) δ 167.3, 167.2, 167.2, 166.1, 163.1, 162.9, 132.9, 132.8, 130.8, 53.8, 53.7, 46.7, 44.9, 42.0, 40.5, 33.0, 32.9, 28.6, 26.7, 21.5, 21.3, 14.3, 12.1. L,L-Isomer: $[\alpha]_{\text{D}}^{25} -18$ (c 1, DMSO).

3-(4-{5-[4-(3-*tert*-Butoxycarbonylacryloylamino)butyl]-3,6-dioxopiperazin-2-yl]butylcarbamoyl}acrylic Acid *tert*-Butyl Ester (9a). A solution of diester **34** (130 mg, 0.44 mmol) in dry THF (10 mL) was added dropwise to a stirring solution of the acetic acid salt of (*R,R*)-diketopiperazine amine **25b** (21 mg, 0.21 mmol), triethylamine (82 mg, 0.79 mmol), and anhydrous Na_2CO_3 (54 mg, 0.51 mmol) in dry THF (10 mL) at rt over a period of 1 h under an N_2 atmosphere. After the addition was complete, the reaction mixture was stirred overnight. The solution was concentrated under vacuum, the residue was dissolved in CH_2Cl_2 (10 mL), and the resultant solid was filtered and washed with CH_2Cl_2 and methanol. The filtrate was concentrated, and the resultant residue was combined with the earlier solid. This crude mixture was then purified by column chromatography using 6% MeOH/0.7% $\text{NH}_4\text{OH}/\text{CH}_2\text{Cl}_2$ to give **9a** in 44% yield: R_f 0.3; ^1H NMR (CDCl_3) δ 6.73 (AB quartet, 4H, CH), 6.22 (br s, 2H, NH), 6.00 (br s, 2H, NH), 4.03 (t, 2H, CH), 3.39 (m, 4H, NCH_2), 1.89 (q, 4H, CH_2), 1.60 (m, 4H, CH_2), 1.49 (m, 22H, CH_3 , CH_2); ^{13}C NMR ($(\text{CD}_3)_2\text{SO}$) δ 167.6, 164.1, 162.6, 136.7, 129.7, 80.9, 54.9, 53.9, 32.8, 28.6, 27.7, 21.8; HRMS (FAB) m/z calcd for $\text{C}_{28}\text{H}_{44}\text{N}_4\text{O}_8$ ($\text{M} + \text{H}$) $^+$ 565.3232, found 565.3218.

Note: For large-scale reaction, the conditions were modified. A solution of **34** (3.43 g, 11.71 mmol) in dry THF (30 mL) was added dropwise to a stirring solution of the acetic acid salt of **25b** (2 g, 5.3 mmol) in aqueous Na_2CO_3 solution

(100 mL, 3.38 g, 31.9 mmol) in THF (50 mL) at 0 °C over a period of 20 min under an N_2 atmosphere. After the addition was complete, the reaction mixture was allowed to stir overnight. The solution was reduced to a 10 mL volume and the solid **9a** precipitated. The solid was filtered, washed with water several times, and dried under high vacuum to obtain **9a** in 80% yield.

3-[[4-(5-[4-[(3-*tert*-Butoxycarbonylacryloyl)ethylamino]butyl]-3,6-dioxopiperazin-2-yl)butyl]ethylcarbamoyl]acrylic Acid *tert*-Butyl Ester (9b). A solution of **34** (5.07 g, 17.31 mmol) in THF (40 mL) was added dropwise to a stirring solution of the acetic acid salt of (*S,S*)-diketopiperazine amine **28** (3.4 g, 7.87 mmol) in aqueous Na_2CO_3 solution (5.0 g, 47.2 mmol) in THF (10 mL) at 0 °C over a period of 20 min under an N_2 atmosphere. After the addition was complete, the reaction mixture was allowed to stir for overnight. THF was evaporated under vacuum, and CH_2Cl_2 (250 mL) was added to the aqueous layer. The aqueous layer was extracted three times with CH_2Cl_2 . The organic layers were combined, dried over Na_2SO_4 , filtered, and concentrated under vacuum. Compound **9b** was purified by column chromatography using 6% MeOH/0.7% $\text{NH}_4\text{OH}/\text{CH}_2\text{Cl}_2$ in 68% yield: R_f 0.4; ^1H NMR (CDCl_3) δ 8.0, 7.89 (1H, NH), 7.24 (d, 2H, CH), 6.70 (d, 2H, CH), 3.97 (br t, 2H, CH), 3.44 (m, 8H, NCH_2), 1.96 (m, 2H, CH_2), 1.82 (m, 2H, CH_2), 1.62 (m, 4H, CH_2), 1.49 (m, 22H, CH_3 , CH_2), 1.21, 1.14 (2t, 6H, CH_3); ^{13}C NMR (CDCl_3) δ 168.9, 168.7, 168.4, 164.8, 164.2, 164.2, 163.9, 133.1, 133.0, 132.9, 132.8, 81.5, 81.5, 54.8, 53.6, 47.6, 45.7, 42.9, 41.5, 34.0, 33.9, 29.4, 28.1, 27.3, 22.3, 15.0, 12.9; HRMS (FAB) m/z calcd for $\text{C}_{32}\text{H}_{52}\text{N}_4\text{O}_8$ ($\text{M} + \text{H}$) $^+$ 621.3858, found 621.3847.

3-(4-{5-[4-(3-*tert*-Butoxycarbonylacryloylamino)butyl]-3,6-dioxopiperazin-2-yl]butylcarbamoyl}acrylic Acid *tert*-Butyl Ester (9c). A solution of diester **34** (1 g, 2.66 mmol) in dry THF (10 mL) was added dropwise to a stirring solution of the acetic acid salt of **35** (1.71 g, 5.84 mmol) in aqueous Na_2CO_3 solution (50 mL, 1.69 g, 15.9 mmol) in THF (75 mL) at 0 °C over a period of 20 min under an N_2 atmosphere. After the addition was complete, the reaction mixture was stirred overnight. The solution was reduced to a 10 mL volume, and the solid **9c** precipitated. The solid was filtered, washed with water several times, and dried under high vacuum to obtain **9c** in 80% yield: ^1H NMR ($(\text{CD}_3)_2\text{SO}$) δ 8.48 (t, 2H, NH), 8.11 (br s, 2H, NH), 6.86 (d, 2H, CH), 6.43 (d, 2H, CH), 3.79 (t, 2H, CH), 3.11 (q, 4H, NCH_2), 1.66 (m, 4H, CH_2), 1.45 (s, 18H, CH_3), 1.42 (m, 4H, CH_2), 1.33 (m, 4H, CH_2); ^{13}C NMR ($(\text{CD}_3)_2\text{SO}$) δ 168.7, 164.9, 163.3, 137.5, 130.5, 81.67, 54.61, 32.8, 29.50, 28.48, 22.21; HRMS (FAB) m/z calcd for $\text{C}_{28}\text{H}_{44}\text{N}_4\text{O}_8$ ($\text{M} + \text{H}$) $^+$ 565.3232, found 565.3230.

3-(4-{5-[4-(3-*tert*-Butoxycarbonylacryloylamino)butyl]-1,4-diethyl-3,6-dioxopiperazin-2-yl]butylcarbamoyl}acrylic Acid *tert*-Butyl Ester (9d). A solution of **34** (4.64 g, 15.8 mmol) in THF (40 mL) was added dropwise to a stirring solution of the acetic acid salt of (*R,R*)-diketopiperazine amine **41** (3.42 g, 6.33 mmol) in aqueous Na_2CO_3 solution (5.37 g, 50.7 mmol) in THF (10 mL) at 0 °C over a period

of 20 min under an N₂ atmosphere. After the addition was complete, the reaction mixture was allowed to stir for overnight. THF was evaporated under vacuum, and CH₂Cl₂ (250 mL) was added to the aqueous layer. The aqueous layer was extracted three times with CH₂Cl₂. The organic layers were combined, dried over Na₂SO₄, filtered, and concentrated under vacuum. Compound **9d** was purified by column chromatography using 4.5% MeOH/CH₂Cl₂ in 87% yield: *R_f* 0.4; ¹H NMR (CDCl₃) δ 7.08 (t, 2H, NH), 6.83 (d, 2H, CH), 6.70 (d, 2H, CH), 3.85 (m, 2H, CH), 3.73 (m, 2H, CH₂), 3.36 (m, 4H, NCH₂), 3.03 (m, 2H, CH₂), 1.93 (m, 2H, CH₂), 1.77 (m, 2H, CH₂), 1.61 (m, 6H, CH₂), 1.49 (m, 20H, CH₃, CH₂), 1.16 (t, 6H, CH₃); ¹³C NMR (CDCl₃) δ 165.6, 164.8, 164.2, 135.7, 131.9, 81.6, 59.8, 40.2, 39.4, 33.5, 28.9, 28.2, 23.4, 12.7; HRMS (FAB) *m/z* calcd for C₃₂H₅₂N₄O₈ (M + H)⁺ 621.3858, found 621.3851.

3-(4-{5-[4-(3-Carboxyacryloylamino)butyl]-1,4-diethyl-3,6-dioxopiperazin-2-yl}butylcarbamoyl)acrylic Acid (9e). A 3.43 g (5.53 mmol) portion of *cis*-di-*tert*-butyl ester **9d** was stirred in 50% TFA/CH₂Cl₂ for 2 h at rt. After the consumption of **9d** was monitored by TLC in 5% MeOH/CH₂Cl₂ (*R_f* = 0.4), the solvents were removed under vacuum. The solid residue obtained was dried under vacuum to obtain white solid **9e** in 98% yield: ¹H NMR ((CD₃)₂SO) δ 8.47 (t, 2H, NH), 6.90 (d, 2H, CH), 6.48 (d, 2H, CH), 3.84 (m, 2H, CH), 3.54 (m, 2H, CH₂), 3.14 (q, 4H, NCH₂), 3.01 (m, 2H, CH₂), 1.79 (m, 2H, CH₂), 1.66 (m, 2H, CH₂), 1.53–1.31 (m, 8H, CH₂), 1.04 (t, 6H, CH₃); ¹³C NMR ((CD₃)₂SO) δ 166.6, 165.2, 163.0, 137.2, 129.4, 59.2, 38.6, 33.1, 28.6, 23.1, 12.5; HRMS (FAB) *m/z* calcd for C₂₄H₃₆N₄O₈ (M + H)⁺ 509.2606, found 509.2582.

6-(3-Ethoxycarbonylacryloylamino)hexanoic Acid (12). A solution of **10** (500 mg, 1.9 mmol) in dry THF (15 mL) was added dropwise to a stirring suspension of 1,6-diaminohexanoic acid **11** (272 mg, 2.1 mmol) and anhydrous Na₂CO₃ (220 mg, 2.1 mmol) in dry THF (10 mL) at rt over a period of 1 h (under a N₂ atmosphere). After the addition was complete, the reaction mixture was stirred overnight. After the consumption of **10** was checked by TLC (*R_f* 0.35 in 60% CH₂Cl₂/hexane), the solution was filtered and concentrated. The residue was dissolved in CH₂Cl₂ (40 mL) and washed three times with aqueous sodium carbonate. The organic layer was separated, dried with anhydrous Na₂SO₄, filtered, and concentrated under vacuum to give a white solid **12**, which was further purified by column chromatography using 5% MeOH/CH₂Cl₂. Washing of the solid with cold CHCl₃ gave pure **12** as a white solid in 62% yield: *R_f* 0.3 in 5% MeOH/CH₂Cl₂; ¹H NMR (CDCl₃) δ 6.81 (q, 2H, CH), 5.84 (br s, 1H, NH), 4.24 (q, 2H, OCH₂), 3.36 (q, 2H, NCH₂), 2.36 (t, 2H, COCH₂), 1.65 (q, 2H, CH₂), 1.59 (q, 2H, CH₂), 1.41 (q, 2H, CH₂), 1.31 (t, 3H, CH₃); ¹³C NMR (CDCl₃ at 60 °C) δ 165.6, 163.8, 136.3, 130.6, 61.3, 39.9, 33.4, 29.3, 26.5, 24.5, 14.4; HRMS (FAB) *m/z* calcd for C₁₂H₁₉NO₅ (M + H)⁺ 258.1336, found 258.1334.

(5-Aminopentyl)carbamic Acid *tert*-Butyl Ester (14). A solution of 1,5-diaminopentane (**13**, 1.8 g, 17.8 mmol) in triethylamine/MeOH (1:7 v/v, 150 mL) was stirred at 0 °C

for 10 min. A solution of di-*tert*-butyl dicarbonate (1.15 g, 5.3 mmol) in MeOH (50 mL) was added dropwise over 10 min. The mixture was stirred for 1 h under a N₂ atmosphere. The temperature was allowed to gradually rise to room temperature, and the solution was stirred overnight. The solution was then evaporated under reduced pressure, and the residue was dissolved in CH₂Cl₂ and washed with deionized water. The organic layer was separated, dried over anhydrous Na₂SO₄, filtered, and concentrated to give a clear oil **14** (92%) that was used in the next step without further purification: *R_f* = 0.35 (12% MeOH/1% NH₄OH/CH₂Cl₂); ¹H NMR (CDCl₃) δ 5.19 (br t, 1H, NH), 3.09 (q, 2H, NHCH₂), 2.68 (t, 2H, NCH₂), 1.29–1.55 (m, 15H, CH₂, CH₃); ¹³C NMR (CDCl₃) δ 155.8, 78.5, 41.9, 40.3, 33.2, 29.8, 28.4, 24.0.

(5-Acetylaminopentyl)carbamic Acid *tert*-Butyl Ester (15). Anhydrous K₂CO₃ (809 mg, 6 mmol) and tetrabutylammonium hydrogen sulfate (TBAHSO₄, 42 mg, 0.14 mmol) were added to compound **14** (409.4 mg, 2.03 mmol) in CH₂Cl₂ (20 mL). Acetyl chloride (785 mg, 10 mmol) in CH₂Cl₂ (10 mL) was then added dropwise to the stirring mixture solution. The reaction was stirred overnight. After the consumption of compound **14** (0.6% NH₄OH/12% MeOH/CH₂Cl₂) was checked, the solution was filtered and concentrated. The residue obtained was dissolved in CH₂Cl₂ (20 mL) and washed two times with a saturated sodium carbonate solution. The organic layer was separated, dried with anhydrous sodium sulfate, filtered, and concentrated to give a residue, which was further purified by column chromatography (0.6% NH₄OH/6% MeOH/CH₂Cl₂) to give pure **15** in 75% yield: *R_f* = 0.31; ¹H NMR (CDCl₃) δ 5.99 (s, 1H, NHBoc), 4.70 (s, 1H, NH), 3.22 (q, 2H, NCH₂), 3.12 (q, 2H, NCH₂), 1.97 (s, 3H, CH₃), 1.44 (m, 15H, CH₃, CH₂); ¹³C NMR (CDCl₃) δ 170.4, 156.3, 79.4, 40.5, 39.8, 30.1, 29.4, 28.8, 24.3, 23.6.

***N*-(5-Aminopentyl)acetamide HCl Salt (16).** HCl (4 N, 8 mL) was added to a solution of **15** (120 mg, 0.49 mmol) in EtOH (4 mL) at 0 °C. After 30 min, the ice bath was removed, and the reaction mixture was allowed to stir overnight under N₂. The mixture was concentrated under high vacuum to give compound **16** in 91% yield.

5-(Ethylaminopentyl)carbamic Acid *tert*-Butyl Ester (17). **Method I.** Bromoethane (77 mg, 0.711 mmol) was dissolved in anhydrous acetonitrile and added to a stirred mixture of amine **14** (286 mg, 1.41 mmol) and anhydrous K₂CO₃ (190 mg, 1.41 mmol). The mixture was then stirred at rt under a N₂ atmosphere overnight. After the disappearance of the ethyl bromide was confirmed by ¹H NMR, the solution was filtered, and the filtrate was concentrated under reduced pressure. The residue was dissolved in CH₂Cl₂ (20 mL) and washed three times with aqueous sodium carbonate (10 wt %). The organic layer was separated, dried with anhydrous Na₂SO₄, filtered, and concentrated under vacuum. Flash column chromatography of the residue (10% MeOH/1% NH₄OH/CH₂Cl₂) gave a mixture of monoBoc monoethylated compound **17** and **14**. Further chromatography in 8.5% MeOH/1% NH₄OH/CH₂Cl₂ provided pure **17** in 61% yield: *R_f* = 0.30 (10% MeOH/1% NH₄OH/CH₂Cl₂); ¹H NMR

(CDCl₃) δ 4.97 (br t, 1H, NH), 3.10 (q, 2H, NHCH₂), 2.63 (m, 4H, NCH₂), 1.30–1.57 (m, 15H, CH₂, BocCH₃), 1.11 (t, 3H, CH₃); ¹³C NMR (CDCl₃) δ 155.9, 78.8, 49.7, 44.1, 40.5, 30.0, 29.8, 28.5, 24.7, 15.3.

Method II. An alternative method (method II) was devised in order to avoid the tedious separation of amines **14** and **17** in method I above. Pd on charcoal (20 wt %, 168 mg) was added to a stirring solution of benzylamine **21** in EtOH (30 mL). The flask was briefly evacuated and H₂ gas admitted via a balloon. The reaction mixture was stirred overnight. After the consumption of compound **21** was checked, the solution was filtered through Celite 521 and concentrated. The residue was dissolved in CH₂Cl₂ (30 mL) and washed two times with a saturated sodium carbonate solution. The organic layer was separated, dried over anhydrous sodium sulfate, filtered, and concentrated to give compound **17** in 90% yield.

3-[(5-*tert*-Butoxycarbonylamino)pentyl]ethylcarbamoylethylacrylic Acid Ethyl Ester (18**).** Separate solutions of **10** (96 mg, 0.36 mmol) and amine **17** (83 mg, 0.36 mmol) each in dry THF (10 mL) were simultaneously added dropwise to a stirring solution of anhydrous Na₂CO₃ (38 mg, 0.36 mmol) in dry THF (10 mL) at –60 °C over a period of 1 h under an N₂ atmosphere. After the addition was complete, the reaction mixture was allowed to stir overnight. After the consumption of **10** was checked by TLC (*R*_f 0.35 in 60% CH₂Cl₂/hexane), the solution was filtered and concentrated. The residue was dissolved in CH₂Cl₂ (40 mL) and washed three times with aqueous sodium carbonate. The organic layer was separated, dried over anhydrous Na₂SO₄, filtered, and concentrated under vacuum to give a pale yellow oil, which was further purified by column chromatography using 2% MeOH/CH₂Cl₂ to give **18**: yield 80%; *R*_f 0.3, 2% MeOH/CH₂Cl₂; ¹H NMR (CDCl₃) δ 7.32 (m, 1H, CH), 6.80 (m, 1H, CH), 4.62 (brs, 1H, NH), 4.24 (q, 2H, OCH₂), 3.40 (m, 4H, NCH₂), 3.13 (q, 2H, NCH₂), 1.47–1.67 (m, 4H, CH₂), 1.44 (m, 9H, CH₃), 1.12–1.39 (m, 8H, CH₂, CH₃); ¹³C NMR (CDCl₃) δ 165.8, 164.1, 163.9, 156.0, 134.0, 133.9, 131.3, 131.2, 79.1, 61.3, 47.9, 46.0, 43.0, 41.6, 40.5, 30.0, 29.8, 29.6, 28.6, 27.6, 24.2, 24.1, 15.2, 14.4, 13.1; HRMS (FAB) *m/z* calcd for C₁₈H₃₂N₂O₅ (M + H)⁺ 357.2384, found 357.2378.

3-[(5-Aminopentyl)ethylcarbamoylethylacrylic Acid Ethyl Ester Trifluoroacetic Acid Salt (19**).** A solution of Boc-protected **18** (86 mg, 0.25 mmol) was dissolved in CH₂Cl₂ (5 mL) and stirred at 0 °C for 10 min. Trifluoroacetic acid (TFA, 5 mL) was added dropwise to the reaction mixture and the solution stirred at 0 °C for 20 min and then at room temperature overnight. The solution was concentrated *in vacuo* to give **19** as a viscous oil in 99% yield: ¹H NMR (CDCl₃) δ 7.29 (m, 1H, CH), 6.70 (m, 1H, CH), 4.22 (m, 2H, OCH₂), 3.40 (m, 4H, NCH₂), 2.97 (m, 2H, NCH₂), 1.71 (m, 2H, CH₂), 1.58 (m, 2H, CH₂), 1.08–1.33 (m, 8H, CH₂, CH₃).

5-(Benzylaminopentyl)carbamic Acid *tert*-Butyl Ester (20**).** Benzaldehyde (0.79 g, 7.4 mmol) was added dropwise to a stirring solution of amine **14** (1.5 g, 7.4 mmol) in 25% MeOH/CH₂Cl₂ (40 mL). The reaction mixture was stirred

overnight under N₂. After the consumption of **14** was checked by TLC (12% MeOH/CH₂Cl₂), NaBH₄ (0.3 g, 8.1 mmol) was added to the vigorously stirred mixture. After 2 h, the reaction was filtered, and the filtrate was concentrated. The residue was dissolved in CH₂Cl₂ (20 mL) and washed two times with a saturated sodium carbonate solution. The organic layer was separated, dried over anhydrous sodium sulfate, filtered, and concentrated to give a residue. Column chromatography using 6% MeOH/CH₂Cl₂ gave pure **20** in 68% yield: *R*_f = 0.32; ¹H NMR (CDCl₃) δ 7.21 (m, 5H, aromatic H), 4.75 (s, 1H, NHBoc), 3.77 (s, 2H, CH₂C₆H₅), 3.29 (s, 1H, NH), 3.07 (q, 2H, NCH₂), 2.61 (t, 2H, NCH₂), 1.43 (m, 13H, CH₃, CH₂), 1.31 (q, 2H, CH₂); ¹³C NMR (CDCl₃) δ 156.2, 139.5, 128.6, 128.5, 127.3, 79.2, 53.9, 49.1, 40.8, 30.2, 29.6, 28.8, 24.8.

[5-(Ethylphenylamino)pentyl]carbamic Acid *tert*-Butyl Ester (21**).** Ethyl bromide (EtBr, 1.52 g, 14 mmol) in CH₃CN (20 mL) was added dropwise to a stirring solution of **20** (0.84 g, 2.88 mmol) and K₂CO₃ (1.88 g, 14 mmol) suspended in CH₃CN (60 mL). The reaction mixture was then allowed to reflux at 60 °C overnight. After the consumption of **20** was checked by TLC (6% MeOH/CH₂Cl₂), the solution was filtered and concentrated. The residue was dissolved in CH₂Cl₂ (30 mL) and washed two times with a saturated sodium carbonate solution. The organic layer was separated, dried over anhydrous sodium sulfate, filtered, and concentrated to give a residue, which was further purified by column chromatography using 0.3% NH₄OH/3% MeOH/CH₂Cl₂ to give pure compound **21** in 95% yield: *R*_f = 0.34; ¹H NMR (CDCl₃) δ 7.22 (m, 5H, aromatic H), 4.56 (s, 1H, NHBoc), 3.53 (s, 2H, CH₂C₆H₅), 3.07 (q, 2H, NCH₂), 2.48 (q, 2H, NCH₂), 2.39 (t, 3H, CH₃), 1.43 (m, 13H, CH₃, CH₂), 1.28 (q, 2H, CH₂); ¹³C NMR (CDCl₃) δ 156.1, 140.1, 129.1, 128.3, 126.9, 79.2, 58.4, 53.3, 47.6, 40.9, 30.3, 28.8, 27.0, 24.9, 12.1.

[5-(Acetyethylamino)pentyl]carbamic Acid *tert*-Butyl Ester (22a**).** Anhydrous K₂CO₃ (501 mg, 3.72 mmol) and tetrabutylammonium hydrogen sulfate (TBAS, 35 mg, 0.1 mmol) were added to compound **17** (285 mg, 1.24 mmol) in CH₂Cl₂ (20 mL). Acetyl chloride (486 mg, 6.2 mmol) in CH₂Cl₂ (10 mL) was then added dropwise to the stirring mixture. The reaction was stirred overnight. After the consumption of compound **17** was checked by TLC (0.6% NH₄OH/12% MeOH/CH₂Cl₂), the reaction mixture was filtered and the filtrate was concentrated. The residue obtained was dissolved in CH₂Cl₂ (20 mL) and washed two times with a saturated aq Na₂CO₃ solution. The organic layer was separated, dried with anhydrous Na₂SO₄, filtered, and concentrated to give a residue, which was further purified by column chromatography (3.5% MeOH/CH₂Cl₂) to give pure acetamide **22a** in 65% yield: *R*_f = 0.35; ¹H NMR (CDCl₃) δ 4.68 (s, 1H, NHBoc), 3.24 (q, 2H, CH₂), 3.16 (t, 2H, CH₂), 3.06 (t, 2H, NCH₂), 2.01 (t, 3H, CH₃), 1.39 (m, 13H, CH₃, CH₂), 1.26 (q, 2H, CH₂), 1.12 (t, 3H, CH₃), 1.05 (t, 3H, CH₃). Note: conformational issues created a complex ¹³C NMR spectrum (CDCl₃): δ 170.1, 169.9, 156.1, 79.3,

79.1, 48.6, 45.2, 43.5, 40.7, 30.3, 30.0, 29.0, 28.7, 28.4, 27.8, 24.4, 21.9, 21.8, 14.4, 13.3.

***N*-(5-Aminopentyl)-*N*-ethylacetamide TFA Salt (22b).** TFA (5 mL) was added dropwise to stirring **22a** (67 mg, 0.25 mmol) in CH₂Cl₂ (5 mL) at 0 °C. After 30 min, the ice bath was removed and the reaction mixture was stirred overnight. After the consumption of **22a**, the reaction solution was filtered and concentrated under high vacuum to give compound **22b** in 77% yield: $R_f = 0.31$ in 0.6% NH₄OH/12% MeOH/CH₂Cl₂; ¹H NMR (CDCl₃): δ 11.01 (s, 1H), 7.82 (d, 2H, NH₂), 3.32 (q, 4H, NCH₂), 2.98 (s, 2H, NCH₂), 2.06 (t, 3H, CH₃), 1.63 (m, 4H, CH₂), 1.25 (m, 5H, CH₃, CH₂).

(6-Benzyloxycarbonylamino-2-*tert*-butoxycarbonylamino)hexanoylamino)acetic Acid Ethyl Ester (23a). *N*^α-*t*-Boc-*N*^ε-Cbz-L-lysine (2 g, 5.26 mmol) was added to a stirred solution of glycine ethyl ester (0.81 g, 7.90 mmol) and *N*-methylmorpholine (1 equiv, NMM) in CH₂Cl₂. The mixture was cooled to 0 °C and DCC (1.63 g, 7.90 mmol) was added in one portion with stirring. The reaction mixture was stirred overnight under a N₂ atmosphere. After the consumption of *N*^α-*t*-Boc-*N*^ε-Cbz-L-lysine was checked by TLC, the solid precipitate (dicyclohexylurea) was filtered off. The filtrate was washed three times with aqueous sodium carbonate. The organic layer was separated, dried over anhydrous Na₂SO₄, filtered, and concentrated under vacuum to give an oil, which was further purified by column chromatography using 1% MeOH/CH₂Cl₂ to give **23a** in 64% yield: ¹H NMR (CDCl₃) δ 7.32 (m, 5H, ArH), 6.94 (br t, 1H, NH), 5.38 (d, 1H, NH), 5.18 (t, 1H, NH), 5.08 (s, 2H, CH₂), 4.18 (m, 3H, CH₂, CH), 3.95 (m, 2H, CH₂), 3.19 (q, 2H, CH₂), 1.82 (q, 1H, CH₂), 1.62 (m, 1H, CH₂), 1.58–1.32 (m, 13H, CH₂, CH₃), 1.24 (t, 3H, CH₃); ¹³C NMR (CDCl₃) δ 172.7, 169.7, 156.6, 155.7, 136.6, 128.4, 127.9, 79.9, 66.6, 61.5, 54.2, 41.3, 40.5, 32.2, 29.4, 28.4, 22.5, 14.2.

[4-(3,6-Dioxopiperazin-2-yl)butyl]carbamic Acid Benzyl Ester (23b). TFA (5 mL) was added dropwise to a stirred solution of **23a** (1.28 g, 2.83 mmol) in CH₂Cl₂ (5 mL) at 0 °C. After 30 min, the ice bath was removed, and the reaction mixture was stirred overnight. After the consumption of **23a** was checked, the solution was concentrated under high vacuum to give the TFA salt, which was further used as crude in next step. 1-Butanol (20 mL) and acetic acid (1 mL) were added to the TFA salt, and a white slurry was observed. NMM (2 mL) was added to the white slurry, and the reaction mixture was refluxed overnight. The reaction mixture became transparent once the reflux started. After 18 h, the reaction mixture was cooled to room temperature and a solid precipitated. The solid (crude **23b**) was filtered and washed with 2-butanol (20 mL) and then with water (20 mL). The white solid was dried under high vacuum to obtain compound **23b** in 95% yield: ¹H NMR ((CD₃)₂SO) δ 8.15 (s, 1H, NH), 7.99 (s, 1H, NH), 7.33 (m, 5H, ArH), 7.25 (t, 1H, NH), 4.99 (s, 2H, CH₂), 3.81–3.60 (m, 3H, CH₂, CH), 2.97 (q, 2H, NCH₂), 1.65 (q, 2H, CH₂), 1.42–1.24 (m, 4H, CH₂); ¹³C NMR ((CD₃)₂SO) δ 167.8, 165.9, 155.9, 137.1, 128.2, 127.6, 65.1, 61.1, 54.1, 44.3, 32.5, 29.2, 21.4.

3-(4-Aminobutyl)piperazine-2,5-dione, Acetic Acid Salt (23c). Pd on charcoal (20 wt %, 0.48 g) was added to a stirred solution of Cbz-protected diketopiperazine of L-Lys **23b** (2.38 g, 0.80 mmol) in 50% acetic acid/CH₂Cl₂ (25 mL). The flask was briefly evacuated, and H₂ gas was admitted via a balloon. The reaction mixture was stirred overnight under a H₂ atmosphere at room temperature. The black suspension was then filtered through a layer of Celite, which was washed several times with MeOH. The combined filtrates were evaporated, and compound **23c** was obtained as a viscous oil, which solidified upon the addition of ethyl acetate. The solid was washed many times with ethyl acetate to obtain the acetic acid salt **23c** in 95% yield: ¹H NMR (D₂O) δ 4.18–3.95 (m, 3H, CH₂, CH), 3.00 (t, 2H, NCH₂), 1.93 (s, 3H, CH₃), 1.80 (m, 2H, CH₂), 1.71 (q, 2H, CH₂), 1.46 (m, 2H, CH₂); ¹³C NMR (D₂O) δ 181.0, 170.3, 168.5, 54.4, 43.9, 39.4, 32.6, 26.7, 23.3, 20.8.

{4-[5-(4-Benzyloxycarbonylamino)butyl]-3,6-dioxopiperazin-2-yl}butyl}carbamic Acid Benzyl Ester (24b). To a stirring solution of Boc-*N*^ε-Z-D-lysine **36** (25 g, 65.8 mmol) in dry THF (100 mL) was added *N*-hydroxysuccinimide (9.08 g, 78.9 mmol). The solution was stirred at 0 °C, and dicyclohexylcarbodiimide (DCC, 16.3 g, 78.9 mmol) was added over a 15 min period. After 15 min of additional stirring at 0 °C, the ice bath was removed, and the solution was stirred at rt overnight. The reaction was monitored by TLC. The solution was filtered and the filtrate concentrated. Dry EtOAc was added, swirled, and filtered and the filtrate concentrated to give the crude *N*-hydroxysuccinimide (NHS) ester **37** as a viscous semisolid. Three volumes of dichloroethane were added to the semisolid to precipitate DCU, the solution was filtered, and the filtrate was concentrated. TFA (50 mL) was added dropwise to the *N*-hydroxysuccinimide (NHS) ester at 0 °C. The reaction was warmed to rt and stirred for 3 h. The volatiles were removed under reduced pressure, and TFA salt was obtained. TFA salt was diluted with 100 mL of dichloroethane and added to 700 mL of pyridine slowly at 0 °C. The solution was slowly allowed to warm to rt and stirred overnight. The volatiles were removed under reduced pressure, and a white solid was obtained, which was washed with EtOAc, MeOH, and water to yield 69% of **24b**: ¹H NMR ((CD₃)₂SO): δ 8.08 (s, 2H, NH), 7.32 (m, 10H, ArH), 7.28 (t, 2H, NH), 3.78 (t, 2H, CH), 2.97 (q, 4H, CH₂), 1.65 (m, 4H, CH₂), 1.37 (t, 8H, CH₂).

(*S,S*)-3,6-Bis(4-aminobutyl)piperazine-2,5-dione, Acetic Acid Salt (25a). Pd on charcoal (20 wt %, 80 mg) was added to a stirring solution of the Cbz-protected diketopiperazine of L-Lys **24a** (400 mg, 0.80 mmol) in 50% acetic acid/CH₂Cl₂ (25 mL). The flask was briefly evacuated and H₂ gas admitted via a balloon. The reaction mixture was allowed to stir overnight under a H₂ atmosphere at room temperature. The black suspension was then filtered through a layer of Celite, which was washed several times with MeOH. The combined filtrates were evaporated, and compound **25a** was obtained as a pale yellow viscous oil, which was solidified by adding ethyl acetate. The solid was washed many times with ethyl acetate to obtain the (*S,S*)-salt **25a** in 96% yield: ¹H NMR

(D₂O) δ 4.16 (t, 2H, CH), 3.01 (t, 4H, NCH₂), 2.00 (s, 6H, 2CH₃), 1.86 (q, 4H, CH₂), 1.71 (q, 4H, CH₂), 1.46 (m, 4H, CH₂); ¹³C NMR (D₂O) δ 179.3, 170.4, 54.3, 39.2, 33.0, 26.5, 22.0, 21.3.

(*R,R*)-3,6-Bis(4-aminobutyl)piperazine-2,5-dione, Acetic Acid Salt (25b). Pd on charcoal (20 wt %, 1.83 g) was added to a stirring solution of the Cbz-protected diketopiperazine of D-Lys **24b** (9.15 g, 17.5 mmol) in 50% acetic acid/CH₂Cl₂ (650 mL). The flask was briefly evacuated and H₂ gas admitted via a balloon. The reaction mixture was allowed to stir overnight under a H₂ atmosphere at room temperature. The black suspension was then filtered through a layer of Celite, which was washed several times with MeOH. The combined filtrates were evaporated, and compound **25b** was obtained as a pale yellow viscous oil, which was solidified by addition of ethyl acetate. The solid was washed many times with ethyl acetate to obtain the (*R,R*)-salt **25b** in 96% yield: ¹H NMR (D₂O) δ 4.16 (t, 2H, CH), 3.01 (t, 4H, NCH₂), 2.00 (s, 6H, 2CH₃), 1.86 (q, 4H, CH₂), 1.71 (q, 4H, CH₂), 1.46 (m, 4H, CH₂); ¹³C NMR (D₂O) δ 179.3, 170.4, 54.3, 39.2, 33.0, 26.5, 22.0, 21.3.

(*S,S*)-3,6-Bis(4-benzylaminobutyl)piperazine-2,5-dione (26a). To a stirred solution of (*S,S*)-**25a** (0.218 g, 0.62 mmol) and triethylamine (TEA, 0.232 g, 2.29 mmol) in 25% MeOH/CH₂Cl₂ (15 mL) was added a solution of benzaldehyde (0.121 g, 1.15 mmol) in 25% MeOH/CH₂Cl₂ (10 mL) under a N₂ atmosphere. The mixture was stirred at rt overnight, and the imine formation was complete (as monitored by ¹H NMR). The solvent was removed *in vacuo*. The solid residue was dissolved in 50% MeOH/CH₂Cl₂ (25 mL), and the solution was cooled to 0 °C. NaBH₄ (6.89 mmol) was added in small portions to the solution, and the mixture was stirred at rt overnight. The solvent was removed *in vacuo*, and the solid residue was dissolved in CH₂Cl₂ (30 mL) and washed with aq Na₂CO₃ solution (10% by wt, 3 × 30 mL). The organic layer was separated, dried over anhydrous Na₂SO₄, filtered, and removed *in vacuo* to give an oily residue. The oil was purified by flash column chromatography (10% MeOH/1% NH₄OH/CH₂Cl₂) to yield the (*S,S*)-**26a** as a pale yellow viscous oil (0.21 g, 76%): *R*_f = 0.35 (10% MeOH/1% NH₄OH/CH₂Cl₂); ¹H NMR (CDCl₃) δ 7.48 (br s, 1H, NH), 7.25 (m, 10H, ArH), 3.90 (m, 2H, CH₂), 3.74 (s, 4H, BnCH₂), 2.61 (br t, 4H, NCH₂), 1.89 (m, 2H, CH₂), 1.74 (m, 2H, CH₂), 1.49 (m, 8H, CH₂); ¹³C NMR (CDCl₃) δ 168.7, 140.3, 128.5, 128.2, 127.0, 55.1, 54.2, 49.1, 34.3, 29.7, 22.9.

(*R,R*)-3,6-Bis(4-benzylaminobutyl)piperazine-2,5-dione (26b). Compound **26b** was prepared by using the same procedure as **26a** using **25b** as starting material with identical yield and NMR as its enantiomer, **26a**, above.

3,6-Bis[4-(benzylethylamino)butyl]piperazine-2,5-dione (27). Bromoethane (307 mg, 2.82 mmol) was dissolved in anhydrous acetonitrile and added to a stirred mixture of **26** (190 mg, 0.44 mmol) and anhydrous K₂CO₃ (389 mg, 2.82 mmol). The mixture was then stirred at 60 °C under a N₂ atmosphere overnight. After the confirmation of the disappearance of the **26** by TLC, the solution was concen-

trated under reduced pressure. The residue was dissolved in CH₂Cl₂ (20 mL) and washed three times with aqueous sodium carbonate. The organic layer was separated, dried over anhydrous Na₂SO₄, filtered, and concentrated under vacuum. Flash column chromatography of the residue gave **27** as a light yellow oil: yield 62%; *R*_f = 0.35 (7% MeOH/0.7% NH₄OH/CH₂Cl₂); ¹H NMR (CDCl₃) δ 7.54 (br s, 1H, NH), 7.25 (m, 10H, ArH), 3.87 (m, 2H, CH₂), 3.51 (s, 4H, BnCH₂), 2.45 (m, 8H, NCH₂), 1.86 (m, 2H, CH₂), 1.69 (m, 2H, CH₂), 1.46 (m, 8H, CH₂), 1.00 (t, 6H, CH₃); ¹³C NMR (CDCl₃) δ 168.8, 139.8, 128.6, 128.2, 126.8, 58.2, 55.1, 53.0, 47.4, 34.5, 26.8, 23.1, 12.0.

3,6-Bis(4-ethylaminobutyl)piperazine-2,5-dione Acetic Acid Salt (28). Pd on charcoal (20 wt %, 27 mg) was added to a stirring solution of benzylamine **27** (132 mg, 0.27 mmol) in 50% acetic acid/CH₂Cl₂ (25 mL). The flask was briefly evacuated and H₂ gas admitted via a balloon. The reaction mixture was allowed to stir overnight under a H₂ atmosphere at room temperature. The black suspension was then filtered through a layer of Celite, which was washed several times with MeOH. The combined filtrates were evaporated, and compound **28** was obtained as a pale yellow, viscous oil in 98% yield: ¹H NMR (D₂O) δ 4.15 (t, 2H, CH), 3.06 (m, 8H, NCH₂), 2.00 (s, 6H, 2CH₃), 1.86 (q, 4H, CH₂), 1.70 (q, 4H, CH₂), 1.46 (m, 4H, CH₂), 1.27 (t, 6H, CH₃); ¹³C NMR (D₂O) δ 178.9, 170.2, 54.4, 46.8, 43.0, 33.1, 25.5, 22.0, 21.5, 10.8.

But-2-enedioic Acid *tert*-Butyl Ester Ethyl Ester (31). To a stirring solution of monoethyl fumarate **29** (200 mg, 1.39 mmol) in dry CH₂Cl₂ (10 mL) were added *tert*-butyl alcohol (312 mg, 4.16 mmol) and dimethylaminopyridine (DMAP, 135 mg, 1.11 mmol). The solution was stirred at 0 °C, and dicyclohexylcarbodiimide (DCC, 315 mg, 1.53 mmol) was added over a 15 min period. After 15 min of additional stirring at 0 °C, the ice bath was removed, and the dark brown solution was stirred at rt for 4 h. The dicyclohexylurea precipitate was removed by filtration. The filtrate was successively washed with two 25 mL portions of 0.5 N HCl and two 25 mL portions of saturated Na₂CO₃ solution. The organic layer was separated, dried over anhydrous Na₂SO₄, filtered, and concentrated under vacuum to give a brown solid, which was further purified by column chromatography using 70% CH₂Cl₂ in hexane to give **31** in 77% yield: *R*_f = 0.4, 70% CH₂Cl₂ in hexane; ¹H NMR (CDCl₃) δ 6.78 (s, 2H, CH), 4.23 (q, 2H, OCH₂), 1.52 (s, 9H, CH₃), 1.27 (t, 3H, CH₃); ¹³C NMR (CDCl₃) δ 164.8, 163.8, 135.4, 132.5, 81.6, 61.1, 27.9, 14.1.

But-2-enedioic acid Mono-*tert*-butyl Ester (32). A 1 M aq NaOH solution (3.6 mL, 0.36 mmol) was added to a cold solution (0 °C) of *tert*-butyl ethyl fumarate **31** (70 mg, 0.35 mmol) in THF (20 mL). After 1 h, the solution was acidified with 4 N HCl, and the THF was evaporated under reduced pressure. The aqueous layer was extracted with dichloromethane (3 × 50 mL). The organic layers were separated, combined, dried over anhydrous Na₂SO₄, filtered, and concentrated under vacuum to give a residue, which was further purified by column chromatography using 2% MeOH/CH₂Cl₂ to give **32** as a white solid in 80% yield: *R*_f 0.3, 2%

MeOH/CH₂Cl₂; ¹H NMR (CDCl₃) δ 6.83 (d, 1H, CH), 6.73 (d, 1H, CH), 1.5 (s, 9H, CH₃); ¹³C NMR (CDCl₃) δ 169.6, 163.9, 137.2, 131.9, 82.3, 27.9.

But-2-enedioic Acid *tert*-Butyl Ester 4-Nitrophenyl Ester (34). Mono *tert*-butyl fumarate **32** (100 mg, 0.58 mmol) in THF (5 mL) was added to a two-necked round-bottom flask. The flask was placed under an Ar atmosphere, and TEA (88 mg, 0.87 mmol) was added. The solution was cooled to 14 °C, and *p*-nitrophenyl trifluoroacetate **33** (150 mg, 0.64 mmol) in THF (5 mL) was added slowly via addition funnel over a period of 15 min. The reaction was warmed to rt and stirred for 4 h at rt. The solution was concentrated under reduced pressure, and the resulting residue was dissolved in CH₂Cl₂ and washed with water. The organic layer was separated, dried over Na₂SO₄, filtered, and concentrated under vacuum. The compound **34** was purified by column chromatography using 60% CH₂Cl₂ in hexane in 89% yield: *R*_f = 0.4, 60% CH₂Cl₂ in hexane; ¹H NMR (CDCl₃) δ 8.27 (d, 2H, CH), 7.34 (d, 2H, CH), 6.96 (q, 2H, CH), 1.54 (s, 9H, CH₃); ¹³C NMR (CDCl₃) δ 163.5, 162.7, 154.9, 145.6, 138.5, 130.8, 125.4, 122.4, 82.7, 28.2; HRMS (FAB) *m/z* calcd for C₁₄H₁₅NO₆ (M + H)⁺ 316.0792, found 316.0791.

Note: For large-scale reactions, the product **34** was separated by adding water to the reaction mixture and solid **34** was filtered and washed several times with water.

Benzyl (4-{5-[4-(Benzyl-*tert*-butoxycarbonylamino)butyl]-3,6-dioxopiperazin-2-yl}butyl)carbamic Acid *tert*-Butyl Ester (38). A solution of **26b** (4.5 g, 10.3 mmol) in triethylamine/MeOH (1:7 v/v, 150 mL) was stirred at 0 °C for 10 min. A solution of di-*tert*-butyl dicarbonate (6.63 g, 25.8 mmol) in MeOH (50 mL) was added dropwise over 10 min. The mixture was stirred for 1 h under a N₂ atmosphere. The temperature was allowed to gradually rise to room temperature, and the solution was stirred overnight. The solution was evaporated under reduced pressure, and the residue was dissolved in CH₂Cl₂ and washed with deionized water. The organic layer was separated, dried over anhydrous Na₂SO₄, filtered, and concentrated to give white solid **38** (94%) that was used in the next step without further purification: *R*_f = 0.4 (3% MeOH/CH₂Cl₂); ¹H NMR (CDCl₃) δ 7.36 (br s, 1H, NH), 7.21 (m, 10H, ArH), 4.37 (br s, 4H, 2CH₂), 3.87 (br s, 2H, CH), 3.20–3.10 (m, 4H, NCH₂), 1.88 (m, 2H, CH₂), 1.72 (m, 2H, CH₂), 1.48–1.25 (m, 26H, CH₂, CH₃); ¹³C NMR (CDCl₃) δ 168.7, 155.7, 138.5, 128.5, 127.6, 127.1, 79.9, 54.9, 50.7, 50.1, 34.1, 33.7, 28.6, 27.9, 27.5, 22.6, 22.4; HRMS (FAB) *m/z* calcd for C₃₆H₅₂N₄O₆ (M + Na)⁺ 659.3779, found 659.3776.

Benzyl (4-{5-[4-(Benzyl-*tert*-butoxycarbonylamino)butyl]-1,4-diethyl-3,6-dioxopiperazin-2-yl}butyl)carbamic Acid *tert*-Butyl Ester (39). To the NaH (60% dispersed in mineral oil, 1.55 g, 64.6 mmol) in a three-necked flask was added dry THF (30 mL) under Ar using a syringe. The solution was allowed to stir for 20 min at rt and then cooled to –78 °C. Compound **38** (6.13 g, 9.64 mmol) in dry THF (50 mL) was added to the stirred solution using a syringe. The solution was allowed to warm to rt and stirred for 1 h. Again the solution was cooled to –78 °C, and bromoethane (10 mL,

120 mmol) was added using a syringe. The reaction was allowed to warm to rt and allowed to stir for two nights. After the disappearance of starting material (by TLC), the solution was concentrated under reduced pressure. The residue was redissolved in CH₂Cl₂ and washed with aqueous Na₂CO₃ solution three times. The organic layers were combined and dried over Na₂SO₄, filtered, and concentrated to give a crude white solid, which was purified using column chromatography (1.5% MeOH/CH₂Cl₂) in 70% yield: *R*_f = 0.4 (3% MeOH/CH₂Cl₂); ¹H NMR (CDCl₃) δ 7.30 (m, 10H, ArH), 4.39 (br s, 4H, CH₂), 3.75 (m, 4H, CH, CH₂), 3.13 (m, 4H, CH₂), 2.93 (m, 2H, CH₂), 1.73 (m, 5H, CH₂), 1.50–1.32 (m, 25H, CH₂), 1.13 (t, 6H, CH₃); ¹³C NMR (CDCl₃) δ 165.1, 155.0, 138.1, 127.9, 127.1, 126.6, 79.1, 59.5, 53.3, 50.1, 49.6, 45.7, 39.6, 33.5, 28.1, 27.2, 23.2, 12.2.

{4-[5-(4-*tert*-Butoxycarbonylamino)butyl]-1,4-diethyl-3,6-dioxopiperazin-2-yl}butyl}carbamic Acid *tert*-Butyl Ester (40). Pd on charcoal (20 wt %, 810 mg) was added to a stirring solution of **39** (4.60 g, 6.65 mmol) in EtOH (100 mL). The flask was briefly evacuated and H₂ gas admitted via a balloon. The reaction mixture was allowed to stir overnight under a H₂ atmosphere at room temperature. The black suspension was then filtered through a layer of Celite, which was washed several times with EtOH. The combined filtrates were evaporated, and compound **40** was obtained as a pale yellow, viscous oil in 97% yield: ¹H NMR (CDCl₃) δ 4.66 (br t, 2H, NH), 3.90–3.71 (m, 4H, CH, CH₂), 3.12 (q, 4H, NCH₂), 2.99 (m, 2H, CH₂), 1.90–1.70 (m, 6H, CH₂), 1.59–1.35 (m, 24H, CH₂, CH₃), 1.16 (t, 6H, CH₃); ¹³C NMR (CDCl₃) δ 165.8, 156.1, 79.3, 60.1, 40.3, 40.3, 34.1, 30.1, 28.7, 23.8, 12.8.

3,6-Bis(4-aminobutyl)-1,4-diethylpiperazine-2,5-di-one, TFA Salt (41). TFA (30 mL) was added dropwise to stirring **39** (3.30 g, 6.45 mmol) in CH₂Cl₂ (30 mL) at 0 °C. After 30 min, the ice bath was removed, and the reaction mixture was stirred for 4 h. After the consumption of **40** was checked by NMR, the reaction solution was concentrated under high vacuum to give compound **41** in 98% yield: ¹H NMR ((CD₃)₂SO) δ 7.74 (br s, 2H), 3.84 (q, 2H, CH), 3.60 (m, 2H, CH₂), 3.0 (m, 2H, CH₂), 2.77 (q, 4H, NCH₂), 1.85–1.39 (m, 12H, CH₂), 1.06 (t, 6H, CH₃).

Acknowledgment. We thank Drs. Destardi Moye-Sherman, Andrea Leone-Bay, John Weidner, and Jim Ferguson at MannKind Corp. and Dr. Thomas Selby (UCF Chemistry) for their helpful discussions. In addition, we thank MannKind Corp. for financial support of this work and supply of the synthetic precursors.

Supporting Information Available: ¹H NMR and ¹³C NMR spectra for **1b,c**, **3–9e**, **12**, **14**, **15**, **17–21**, **22a,b**, **23a–c**, **24b**, **25a,b**, **26a,b**, **27**, **28**, **31**, **32**, **34**, and **38–41**; IR spectra for NH (3160–3500 cm^{–1}) and carbonyl (1550–1800 cm^{–1}) regions of **3–9(a–d)**. Elemental analysis of compounds **3–6**, **7a,b**, **8a**, **9a–e**, **12**, **18**, **22a**, **34**, and **38**. This material is available free of charge via the Internet at <http://pubs.acs.org>.

MP700096E